MEASUREMENTS OF COUPLED RAYLEIGH WAVE PROPAGATION IN AN ELASTIC PLATE

BY

BOON WEE TI

B.S., University of Illinois, 1995

THESIS

Submitted in partial fulfilment of the requirements
for the degree of Master of Science in Electrical Engineering
in the Graduate College of the
University of Illinois at Urbana-Champaign, 1997

Urbana, Illinois

UNIVERSITY OF ILLINOIS AT URBANA-CHAMPAIGN

THE GRADUATE COLLEGE

DECEMBER 1996

WE HEREBY RECOMMEND THAT THE THESIS BY

TI BOON WEE

ENTITLED MEASUREMENTS OF COUPLED RAYLEIGH WAVE PROPAGATION IN AN ELASTIC PLATE

BE ACCEPTED IN PARTIAL FULFILLMENT OF THE REQUIREMENTS FOR THE DEGREE OF MASTER OF SCIENCE

W. D'Brien

Director of Thesis Research

N. Narayana Rao

Head of Department

Committee on Final Examination†

Chairperson

† Required for doctor's degree but not for master's.

O-517

ACKNOWLEDGEMENTS

This work is made possible by the support of the American Chemical Society (Petroleum Research Fund) under the guidance of Professors John G. Harris and William D. O'Brien of the University of Illinois at Urbana-Champaign.

TABLE OF CONTENTS

Page

1 INTRODUCTION 1

2 THEORY 3

3 MATERIALS AND METHODOLOGY 5

4 COMPUTER PROGRAMS 12

5 RESULTS 13

6 UNCERTAINITIES 15

7 DISCUSSION 18

8 FUTURE STEPS 20

APPENDIX A DERIVATION OF BEATLENGTH 45

A.1 Introduction 45

A.2 Terms and Definitions 45

A.3 Scalar and Vector Potentials 46

A.4 Displacement Equations 47

A.5 Boundary Conditions 47

A.6 Symmetric Wave Displacements 48

A.7 Brekhovskikh's and Goncharov's Estimate 49

A.8 Asymmetric Wave Displacements 50

A.9 Beatlength 51

APPENDIX B COMPUTER PROGRAMS 53

APPENDIX C EXPERIMENTAL RESULTS 66

LIST OF REFERENCES 83

1 INTRODUCTION

The two lowest waveguide modes of an elastic plate can be described as the propagation of a Rayleigh wave that starts on one surface, but that gradually transfers to the other surface. It then transfers back to the surface from which it started, the whole cycle taking place over a distance we call the beatlength. If the product of the wave number and thickness is sufficiently large, one can thus view a plate as two weakly coupled surface-wave waveguides. The objective of this thesis is to report measurements of the beatlength in aluminum, brass and glass plates. This may be one of the first detailed experimental assessments of this phenomenon, though its possibility has been noted by Auld [1], Viktorov [2] and Brekhovskikh and Goncharov [3].

The longer service lives of structures such as pipelines mean that they must be monitored for damage more thoroughly, and over a longer period of time. Using coupled surface waves may be one way to inspect the inner and, therefore, not easily accessible surface of a pipe from its outer surface. Moreover, if the damage were a small surface-breaking fatigue crack, then a surface wave would readily detect the crack because the surface wave would strike it broadside, or if the damage was due to corrosion, then a surface wave would be more severely attenuated by the patch of corrosion at the surface than a bulk wave. In a similar fashion, coupled surface waves may be advantageous in the inspection of any walled container where the inner wall or the outer wall is not easily accessible or inaccessible. Examples are aircraft frames, sealed containers and ship frames.

The present measurements indicate that the coupled surface waves are readily excited and detected so that they can be used for such non-destructive testing.

2 THEORY

The basic idea is presented graphically. Figure 1 shows the dispersion relation for the two lowest, Rayleigh-Lamb modes (all figures/tables appear at end of thesis). The lower curve is for the lowest antisymmetric mode, while the upper curve is for the lowest symmetric mode. The vertical axis is the normalized angular frequency (ω multiplied by (h/c_t), where h is one-half the thickness of the plate and c_t is the transverse wave speed). The horizontal axis is the normalized x_1-component of the wave number (β multiplied by $\omega h/c_t$). The short dashed line indicates the straight line formed by $\omega h/c_t$ plotted against $\beta_r\ \omega h/c_t$, where β_r is the Rayleigh wave number. The slope is (c_r/c_t), where c_r is the Rayleigh wave speed. In the neighborhood of the intersection points of the long dashed horizontal line with the dispersion curves, the x_1-particle displacements are as sketched in Fig. 2. In Fig. 2(a) the symmetric mode is sketched, in Fig. 2(b) the antisymmetric mode is sketched, and in Fig. 2(c) their algebraic sum is sketched. If the symmetric and antisymmetric modes are both excited in phase, then the sum approximates a Rayleigh wave on the upper surface. This is indicated by the solid line in Fig. 2(c). However, each mode propagates with a slightly different normalized wave number, β_s for the symmetric mode and β_a for the antisymmetric mode. After a distance $L/2$, the two modes move π out of phase. Adding the two modes together at this location approximates a Rayleigh wave on the lower surface, which is indicated by the dashed line in Fig. 2(c). After propagating an additional distance $L/2$, the modes move back into phase (more accurately 2π out of phase) and their sum approximates a Rayleigh wave, this time on the upper surface. In this sense, the propagation of the two

modes can be viewed as a Rayleigh surface wave coupling from one surface-wave waveguide to another. In Fig. 1, the vertical dashed lines indicate the difference 2ε between the normalized wave numbers β_s and β_a. The difference between β_s and β_r is almost equal to that between β_r and β_a. The beatlength, L, of the coupled waves is that distance over which the two modes move out of phase by 2π, that is,

$$\frac{\omega}{c_t}(\beta_a - \beta_s)L = 2\pi \tag{1}$$

or

$$\frac{L}{h} = \frac{\pi c_t}{\omega h \varepsilon} \tag{2}$$

where ε is depicted in Fig. 1. Brekhovskikh and Goncharov [3] give an estimate of ε for large $\beta_r h$. In our project, the exact dispersion relation was used to find β_s, β_a and ε. Appendix A contains a more detailed mathematical derivation of the beatlength.

3 MATERIALS AND METHODOLOGY

Three elastic plates were used: an aluminum plate 30.48 *cm* (1 *ft*) by 60.96 *cm* (2 *ft*) by 2.38 *mm* (3/32 *in*), a brass plate 30.48 *cm* (1 *ft*) by 45.72 *cm* (1.5 *ft*) by 2.38 *mm* (3/32 *in*) and a glass plate 30.48 *cm* (1 *ft*) by 60.96 *cm* (2 *ft*) by 3.18 *mm* (1/8 *in*). The brass and glass plates had no discernible surface coatings, while the aluminum might have had a thin layer of oxide. The elastic plates were used as they were when obtained from the manufacturers. No attempt was made to polish the surfaces or treat the surfaces in any fashion so that the robustness of the beating phenomenon could be ascertained.

The longitudinal wave speed in aluminum, brass and glass was experimentally determined as follows. Figure 3(a) shows the schematic diagram of the setup for measuring the longitudinal speed. A focused 15 *MHz* Panametrics V3619 immersion transducer was placed in the water tank facing the vertically placed elastic plate. The transducer was set up via a Panametrics 5800 Pulser/Receiver, to work in standard pulse-echo mode. The direction of the beam axis perpendicular to the surface of the elastic plate was found by adjusting the focused transducer to an angle at which the reflected ultrasonic signal was maximum. For all other angles, the ultrasonic beam will not be reflected directly back onto the face of the transducer. Hence, for these angles, the reflected signal will be weaker.

The adjustment was controlled by a positioning system that has a linear accuracy of about 5 μm and a rotational accuracy of about 0.02°. Figure 4 shows a photograph of this positioning system, the Daedal MC2000 controller and the Daedal MD23/M34

of this positioning system, the Daedal MC2000 controller and the Daedal MD23/M34 motor drive system. The motor assembly in the center of Fig. 4 consists of the two rotational motors that control motion in the two rotational axes. The Daedal system also allows movement in the three orthogonal directional axes. When the elastic plate is eventually inserted into the water tank as shown in Fig. 3(a), and the positive x_1-axis is the direction pointing out of the figure, the positive x_2-axis is the direction pointing vertically towards the bottom of Fig. 3(a), and the positive x_3-axis is the direction pointing horizontally to the right. On the Daedal MC2000 controller, the x_1-axis is controlled by the panel labelled 'AXIS 1,' the x_2-axis is controlled by the panel labelled 'AXIS 3' and the x_3-axis is controlled by the panel labelled 'AXIS 2'.

The 1024-point data record of the received temporal signals from both the reflection off the near surface and the far surface of the elastic plate were recorded using a Tektronix 11401 oscilloscope, at 500 *MHz* for aluminum and glass and at 200 *MHz* for brass. The effect of changing the sampling frequency will be discussed in Chapter 7. A program written in *Matlab* was then used to find the round-trip time taken for sound to travel between the near and far surfaces of the elastic plate and, subsequently, the longitudinal speed in the elastic plate. The portions of the sampled reflected signal corresponding to the reflections off the two surfaces of the elastic plate were isolated and separated, and the round-trip time taken to travel between the two surfaces, t, was found by finding the maximum correlation coefficient between them.

The wave speed, in each case, is calculated as follows:

$$c = \frac{4h}{t} \tag{3}$$

where c is the shear or longitudinal speed, t, the round-trip time sound takes to travel from one side of the elastic plate to the other side, and $4h$, twice the thickness of the elastic plate, since the thickness is $2h$.

The shear wave speeds in aluminum, brass and glass were subsequently experimentally determined as follows. Figure 3(b) shows the schematic diagram of the setup for measuring the shear speed. The elastic plate was removed from the water, wiped dried and placed horizontally over the water tank. The immersion transducer was replaced by a V222-BA-RM normal incidence shear-wave contact transducer. This transducer has a 7-μs delay line. Clover honey was used as a coupling agent. The coupling agent was prepared as follows. A small amount of clover honey was boiled. A large drop of honey, just large enough to cover the contact surface of the contact transducer, was deposited onto the elastic plate before the honey cooled. The honey was allowed to cool and harden for a minute. Honey was used as a coupling agent because of its high viscosity. At $15^{o}C$, the kinematic viscosity of honey is 1200 compared to 0.01 for water, 1.0 for olive oil and 18 for glycerine. The contact transducer was then pressed into the honey. The 1024-point data record of the received temporal signals from both the reflection off the top surface and the bottom surface of the elastic plate was recorded using a Tektronix 11401 oscilloscope, at 500 *MHz* for aluminum and glass, and at 200 *MHz* for brass. The shear speed was calculated the same way as the longitudinal speed.

With the longitudinal and shear wave speeds and the thickness of the elastic plate, the beatlengths at different transmit frequencies were calculated as follows. A *Mathematica* program calculates the symmetric wave number, β_s, and antisymmetric wave number, β_a at different transmit frequencies. Consequently, β_r and ε can be calculated as follows :

$$\beta_r \approx \beta_{mean} = \frac{\beta_s + \beta_a}{2} \tag{4}$$

$$\varepsilon = \frac{\beta_a - \beta_s}{2} \tag{5}$$

The beatlength, L, and normalized beatlength, L/h, can be calculated using Eq. (2). The spatial beat frequency, f_a, is the reciprocal of L. Additionally, the Rayleigh angle, θ_r is calculated from

$$\theta_r = \sin^{-1}\left(\frac{c_w}{c_r}\right) \tag{6}$$

where c_w is the speed of sound in water. A very good approximation (accurate to within 0.5%) for c_r is [2]

$$\frac{c_r}{c_t} = \frac{(0.87 + 1.12\nu)}{1+\nu} \tag{7}$$

were used to mark the positions of the transmit signal and the reflected signal. To ensure that the direction of the beam axis is perpendicular to the plate surface, the transducer was moved along the x_1-axis and the maximum reflected signal's position on the oscilloscope is monitored. If the plate is not positioned parallel to the x_1-axis, the reflected signal on the oscilloscope will move closer or farther from the transmit signal. The elastic plate is adjusted until the plate is parallel to the x_1-axis. Then, the transducer was moved above water and rotated to the calculated Rayleigh angle, θ_r. The transducer was then moved toward the vertically placed elastic plate until the water jacket just pressed against the plate surface. The water jacket was designed such that its extension beyond the transducer's element surface is the focal length of the transducer. As such, by resting the water-jacket onto the plate surface, the focus can be on the surface of the plate, resulting in the maximum transfer of energy. The transducer was also adjusted such that the transducer was in a horizontal line with the broadband receive transducer, a Deci Model SE 1025-H308 surface contact transducer. At this point, data were ready to be collected.

The beatlength was experimentally determined as follows. With the transmit beam at the Rayleigh angle and the transmit focus on the elastic plate, the transmit transducer was precisely moved parallel to the elastic plate surface, along the x_1-axis, toward the receive transducer. The transmit transducer was moved in $200\,\mu m$ intervals, and at each interval, a 1024-point, 10 *MHz* data record of the temporal, received, sinusoidal signal was recorded by the receive transducer. The sampling rate was judged sufficient because the maximum transmit frequency used was 1.6 *MHz*. The RMS value

of the temporal, received, sinusoidal signal for each position was calculated and recorded. The transmit transducer was moved a total distance at least three times the estimated beatlength. For the range of measured beatlengths, this corresponds to collecting between 150 to 750 RMS values. The RMS data set was Fourier transformed using a 4096 FFT. The power spectrum was calculated to determine a peak in the power spectrum corresponding to the beatlength.

The experiment was repeated for different transmit frequencies for three different materials of varying thicknesses.

4 COMPUTER PROGRAMS

In Appendix B, the computer programs used in this project are collected. They include the data acquisition program, written in C, *rowscan.c*, the *Matlab* program to measure the speed of sound in the elastic plates, *corr.m*, the *Mathematica* program to calculate the wave numbers, *sym.ma*, and the representative *Matlab* program to determine the spatial beat frequency, *b933.m*.

5 RESULTS

The longitudinal wave speeds in the aluminum, brass and glass plates were experimentally determined to be 6902 *m/s*, 4536 *m/s* and 5257 *m/s*, respectively. The correlation coefficients were calculated to be 80.81%, 76.02% and 68.70%, respectively. A correlation coefficient of 100% means that the reflected signals off both surfaces have exactly the same shape. In other words, the reflected signals off both surfaces have the same frequency content. The received signal plots and the correlation coefficient plots are shown in Figs. 6(a) and (b), Figs. 7(a) and (b) and Figs. 8(a) and (b), respectively.

The shear wave speeds in the aluminum, brass and glass plates that were used were experimentally determined to be 3382 *m/s*, 2215 *m/s* and 3199 *m/s*, respectively. The correlation coefficients were calculated to be 98.71%, 91.52% and 90.47%, respectively. The received signal plots and their corresponding correlation coefficient plots are shown in Figs. 9(a) and (b), Figs. 10(a) and (b), and Figs. 11(a) and (b), respectively.

Using Eq. (6), the Rayleigh angles for aluminum, brass and glass were calculated to be 28.92°, 47.58° and 31.53°. These were the angles used in the experiments.

Figures 12, 13 and 14 show typical measurements for aluminum (case 2 of Table 1), brass (case 4 of Table 2) and glass (case 5 of Table 3). Figures 12(a), 13(a) and 14(a) show the spatially, amplitude modulated received signals from 50 *mm*, 100 *mm* and 50 *mm* scans, that is, the transmit transducer moved 50 *mm* or 100 *mm*, at 200 μm

intervals, towards the receive transducer. Figures 12(b), 13(b) and 14(b) show the spatial power spectrums of the signals from Figs. 12(a), 13(a) and 14(a) plotted against the spatial frequency. The vertical lines in Figs. 12(b), 13(b) and 14(b) mark the theoretically predicted spatial beat frequency in each case calculated using the exact dispersion relation [1] and Eq. (1).

The experiment was repeated for five different frequencies with aluminum, seven different frequencies with brass and five different frequencies with glass. The amplitude modulated signals and their power spectrums for these cases are attached in Appendix C.

Figures 15, 16 and 17 plot L/h against $\omega h/c_t$ for aluminum, brass and glass, respectively. Error bars represent ±10% of a theoretically predicted values have been added so that the reader can have some basis of reference.

Tables 4, 5 and 6 summarize the results of the experiments conducted on aluminum, brass and glass, respectively. In all three tables, f, the transmit frequency of the transducer is varied to produce different $\omega h/c_t$ cases. To have a spatially modulated signal, $\beta_r > \varepsilon$. For reference, the ratio β_r/ε is tabulated using the approximation expressed in Eqs. (4) and (5). The theoretical predictions and experimental determinations for f_a, the spatial beat frequency, L, the spatial beatlength, and L/h are tabulated as well.

6 UNCERTAINTIES

There were several assumptions made about the elastic plate that could introduce some degree of uncertainty in our measurements. Also, there are experimental uncertainties associated with the measurements. In this section, the sources of these uncertainties will be identified and quantified where possible. Any steps taken to minimize these uncertainties will also be discussed.

The elastic plates were assumed to be infinitely planar. This was assumed so that the reflections off of the edges need not be considered, and is accurate provided that the beatlength was measured away from the edges at the central region of the plate, and provided that the planar dimensions of the plate were large when compared to the thickness. Because the measurements were made in the x_1-direction, a comparison of the ratio of the size of the elastic plates in the x_1-direction over the thickness, in the x_3-direction, might be revealing. For aluminum, brass and glass, the ratios are 256, 192 and 192, respectively. This suggests that elastic plates can be considered, for practical purposes, to be infinitely planar.

The two surfaces of the elastic plates are also assumed to be parallel and without any surface imperfections. A standard micrometer was used to measure the thickness of the elastic plates. Due to the shape of the micrometer, it was not possible to measure the thickness of the plate at the center of the plate where the beatlength was measured. The thickness of the plate at the corners was measured instead. The average thicknesses of

the aluminum, brass and glass plates were measured to be $2380 \pm 141\,\mu m$, $2381 \pm 121\,\mu m$, and $3175 \pm 54\,\mu m$, respectively.

In the measurement of the longitudinal and shear speeds, there are discretization uncertainties involved. Table 7 summarizes the uncertainties based on Eq. (9) below. The Δc calculated in table 7 will account for both the uncertainty involved in the measurement of the thickness and the discretization uncertainty involved in measuring the round-trip time of sound between the surfaces, *t*,

$$\frac{\Delta c}{c} = \frac{\Delta t}{t} + \frac{2\Delta h}{2h} \tag{9}$$

In the measurements of the beatlength, the transmit transducer used was a focused 3 *MHz* Panametrics V3680 transducer. In this project, the frequencies used were between 700 *kHz* and 1.46 *MHz*. The continuous-wave sinusoidal transmit signal was displayed and its frequency verified on the oscilloscope. There appear to be no problems associated with getting a 3 *MHz* transducer to put out a waveform of a different frequency. The only discernible effect was a variation in amplitude of the transmit signal at different frequencies. As a result, the amplitude of the receiving signal varied with frequencies. Since the amplitude information is not useful, the received signal plots used in determining the beatlength, Figs 12, 13, 14 and Appendix C, were normalized, i.e., the relative amplitude and relative power spectrum were plotted.

The positioning system used has a linear accuracy of about $5\,\mu m$ and rotational accuracy of about 0.02°. There are discretization uncertainties involved since data were

collected at 200 μm intervals. Therefore, the beatlength was determined to be 200 ± 5 μm. The experimental beatlengths that were measured lie between 9.9 *mm* and 45.5 *mm*. This represents an accuracy of between $\pm 0.44\%$ (for L = 45.5 *mm*, the maximum beatlength measured) to $\pm 2\%$ (for L = 9.9 *mm*, the minimum beatlength measured).

7 DISCUSSION

The objectives are to determine whether the beatlength could be measured, and if so, to ascertain how robust the phenomenon is and, finally, to compare how well the experimentally measured beatlength compares to the theoretical beatlength.

Appendix C contains the individual results from the 17 measurements made, five from aluminum, seven from brass and five from glass. A representative case for brass is presented in Fig. 13. Figure 13(a) shows the spatially, amplitude modulated received signal plotted against position along the plate's surface. Figure 13(b) suggests the power spectrum of the signal from Fig. 13(a) plotted against the spatial frequency (1/distance). The vertical line indicates the theoretically estimated spatial beat frequency, $L = \pi c_t / (\varepsilon \omega)$. Figure 13(b) shows that the beat phenomenon is robust in the spatial frequency domain, and in reasonable agreement with theory (see Table 5). The first (extreme left) frequency peak is due to the finite spatial window in Fig. 13(a). The second frequency peak is due to the periodicity between two beatlengths. Naturally the more beatlengths that can fit into the spatial window in Fig. 13(a), the more subharmonics of the beat frequency are likely to appear in Fig. 13(b). The representative cases for aluminum and glass, which are shown in Figs. 12 and 14, are similar to Fig. 13.

Figures 15, 16 and 17 are the plots of L/h against $\omega h / c_t$ for aluminum, brass and glass, respectively. The data points, represented by squares, are the measured results. The data points represented by diamonds are the theoretically predicted results. A $\pm$ 10% error bar is attached to each of the theoretically predicted results to provide a

basis of reference. The plots indicate that the measured values of the beatlength, L/h normalized by the half-thickness of the elastic plate, are close to or within $\pm$ 10% of the theoretically predicted values. Brekhovskikh and Goncharov [3] suggest that $\beta_r h$ must be large and their estimate of ε in Eq. (2) assumes this. However, in this project, the values of $\beta_r h$ ranged from 2 to 5 and yet the coupling phenomenon can be observed without difficulty.

The beatlengths indicate that the use of the coupled waves to access an inner surface is realistic. None of the beatlengths is so great that the signals would become too severely attenuated, with distance, to carry information from the far surface.

Initially, there had been concerns that, in addition to the two lowest modes, the higher modes might be excited and, consequently, some power would be carried by them and lost to the coupling phenomenon. This appears not to be the case, suggesting that when the ultrasound beam is incident at the Rayleigh angle, only the two lowest modes are excited.

8 FUTURE STEPS

In the process of this investigation of the Rayleigh surface-wave phenomenon, several questions suggesting avenues of further research that went unanswered. One such question is how robust is the phenomenon, if we send the transducer beam at angles slightly off the Rayleigh angle? Another question is how far the surface wave can propagate before the received signal becomes undetectable? This is basically an attenuation issue. Another question is: the effects of the size and shape of the focal region of the transducer have on the beatlength? The theory also has to be developed for curved surfaces, so that eventually, experiments can be done on pipelines. It would also be interesting to find how the presence of well-defined discontinuities, i.e. , cracks, affects the received signal.

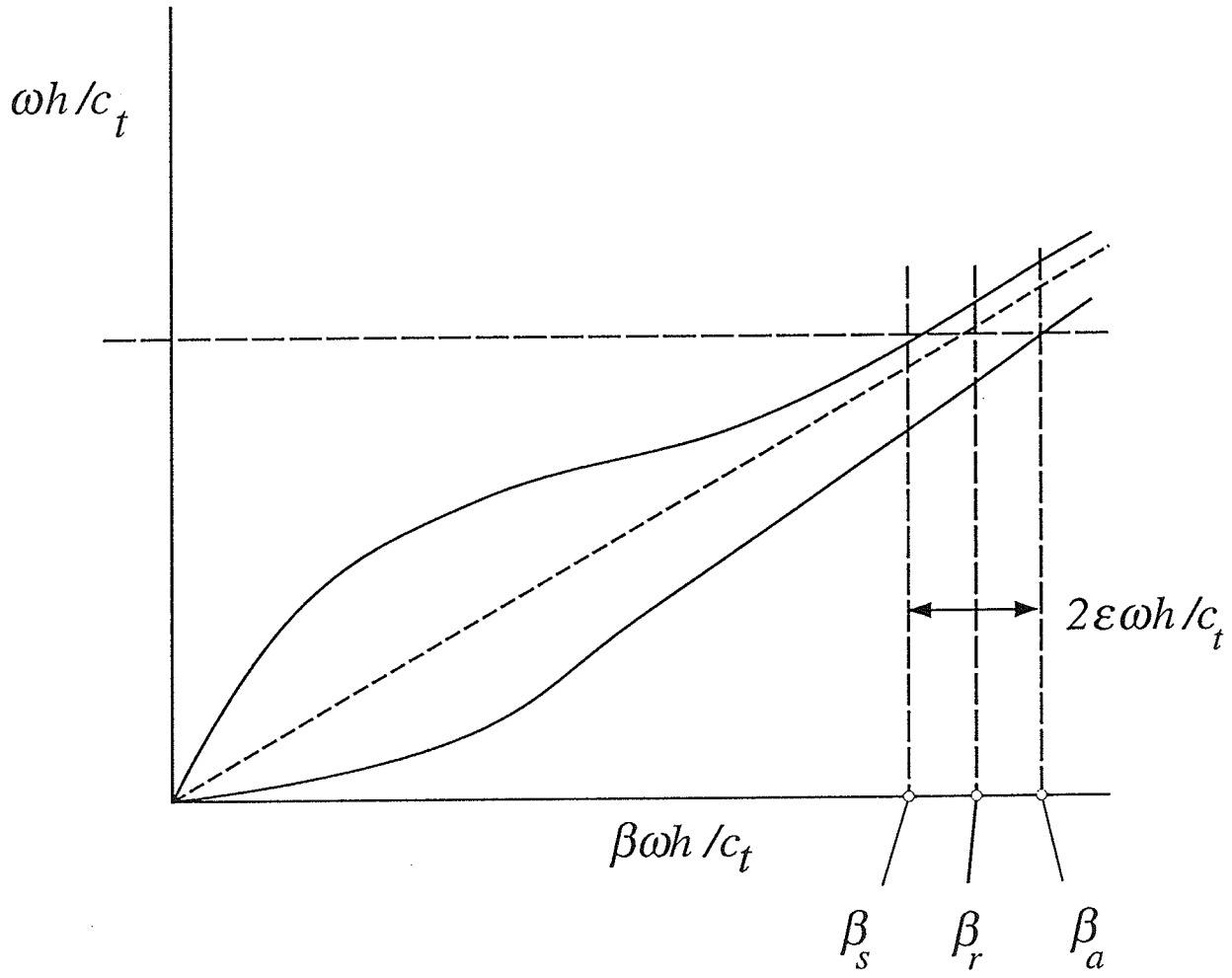

Figure 1. The dispersion relation for the two lowest modes of an elastic plate. The upper curve is the symmetric mode and the lower curve is the anti-symmetric mode. The beatlength $L = \pi c_t / (\varepsilon \omega)$. Figure 2 indicates the particle displacement in the neighbourhood of the intersections of the long dashed horizontal line with the dispersion curves.

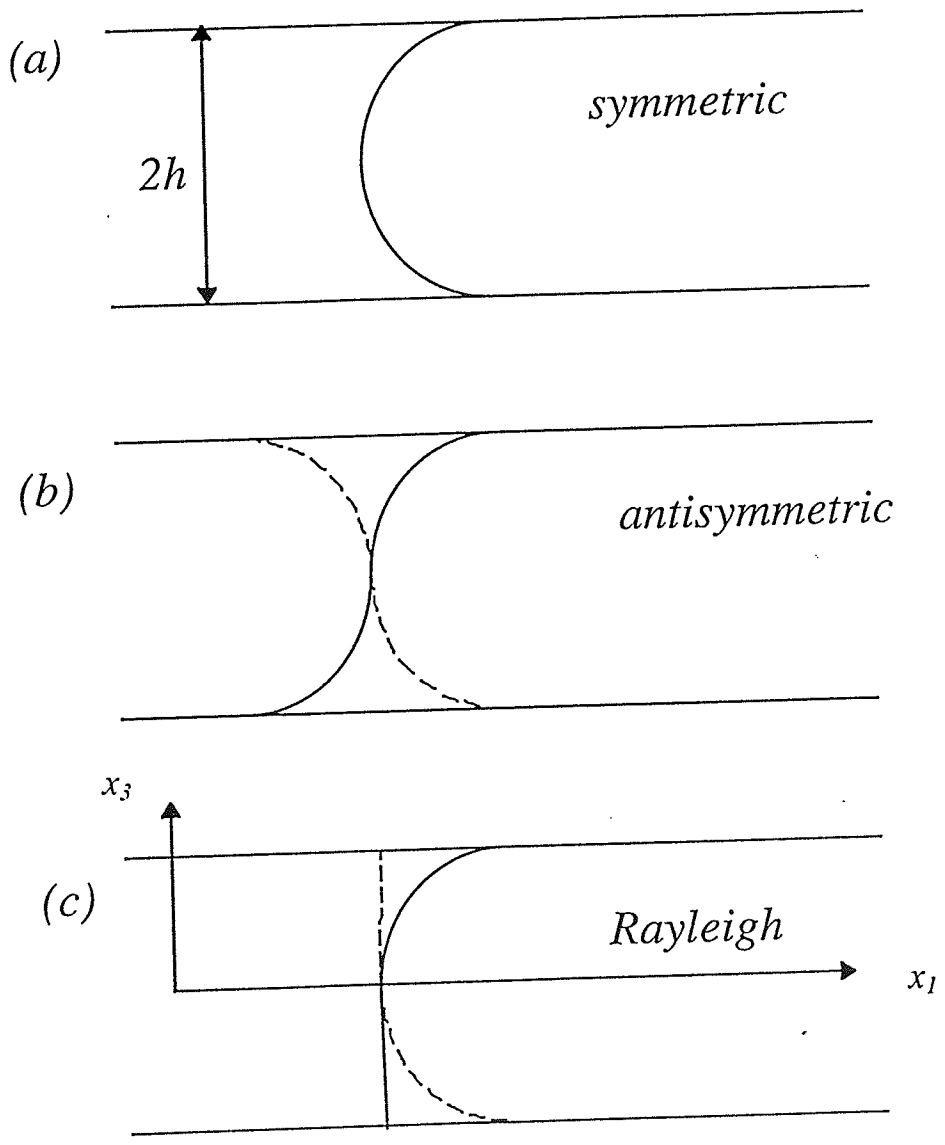

Figure 2. A sketch of the x_1 particle displacements corresponding to the neighbourhood of the intersections of the long dashed horizontal lines in Fig. 1 with the dispersion curves. The solid lines indicate that the modes are in phase, while the dashed lines indicate that they are π out of phase. (a) symmetric mode; (b) antisymmetric mode; (c) algebraic sum of the two modes.

(a)

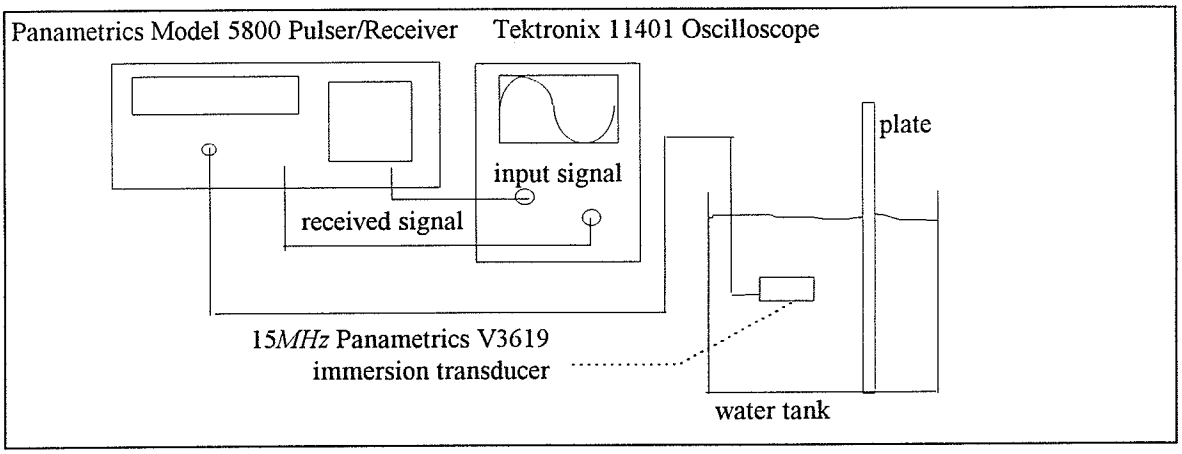

(b)

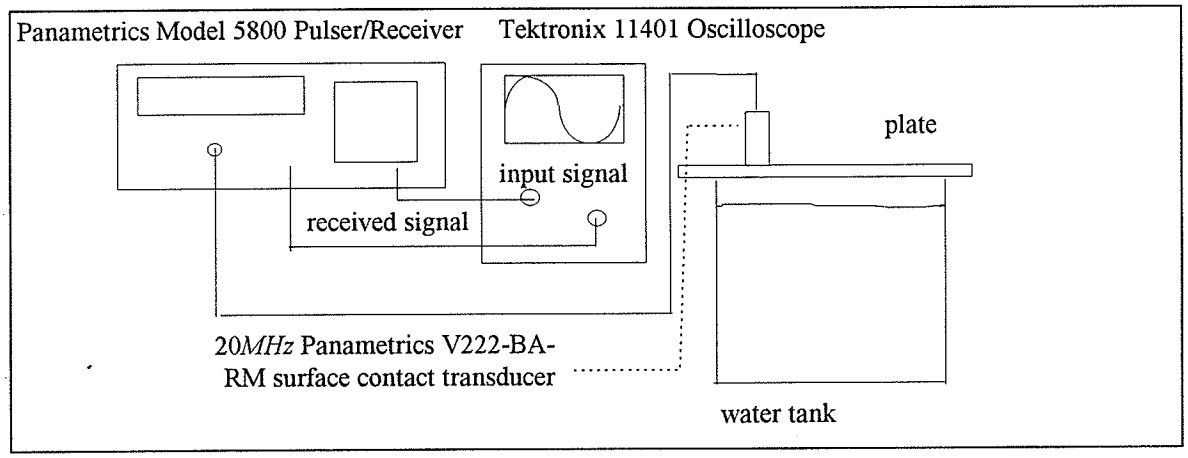

Figure 3. Schematic diagrams of the experimental setup for measuring (a) the longitudinal speed and (b) shear speed in an elastic plate.

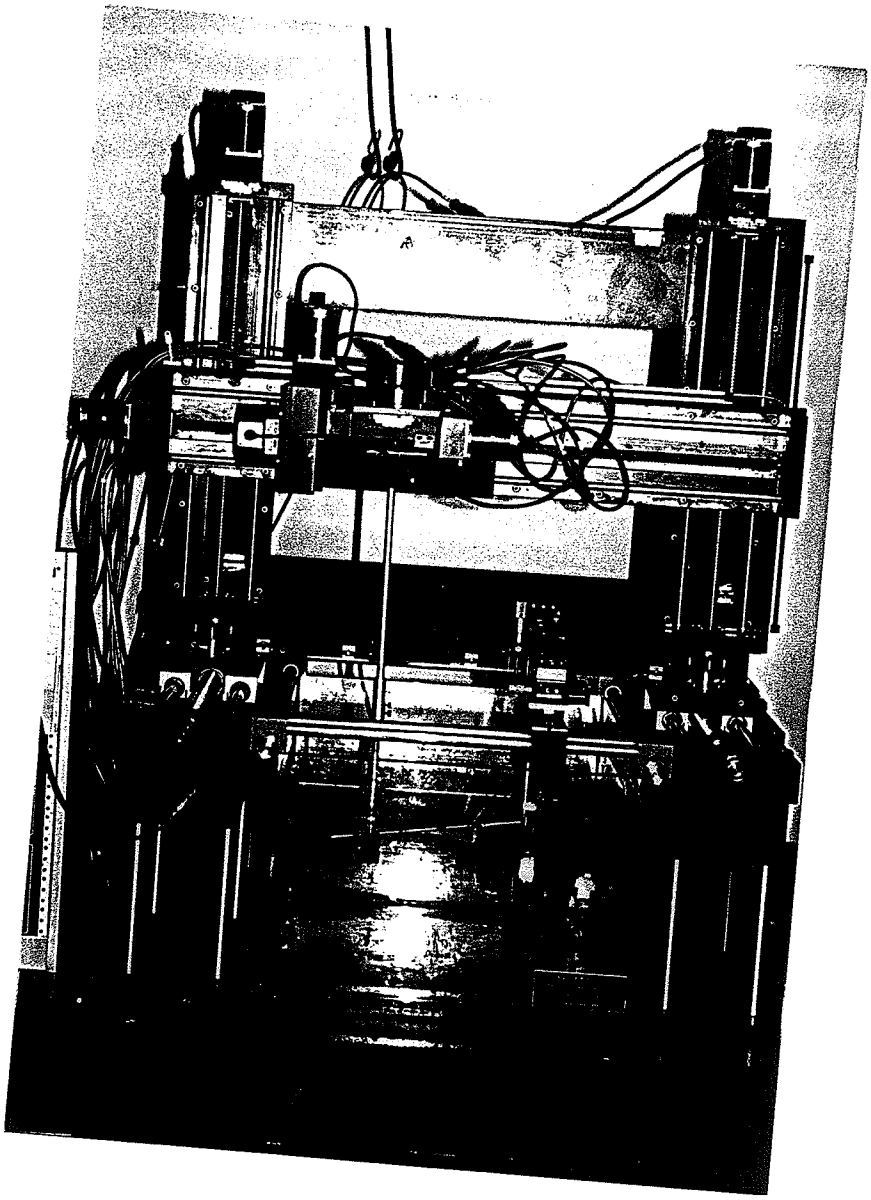

Figure 4. Photograph of the Daedal MC2000 Controller and MD23/ MD34 Motor / Drive System.

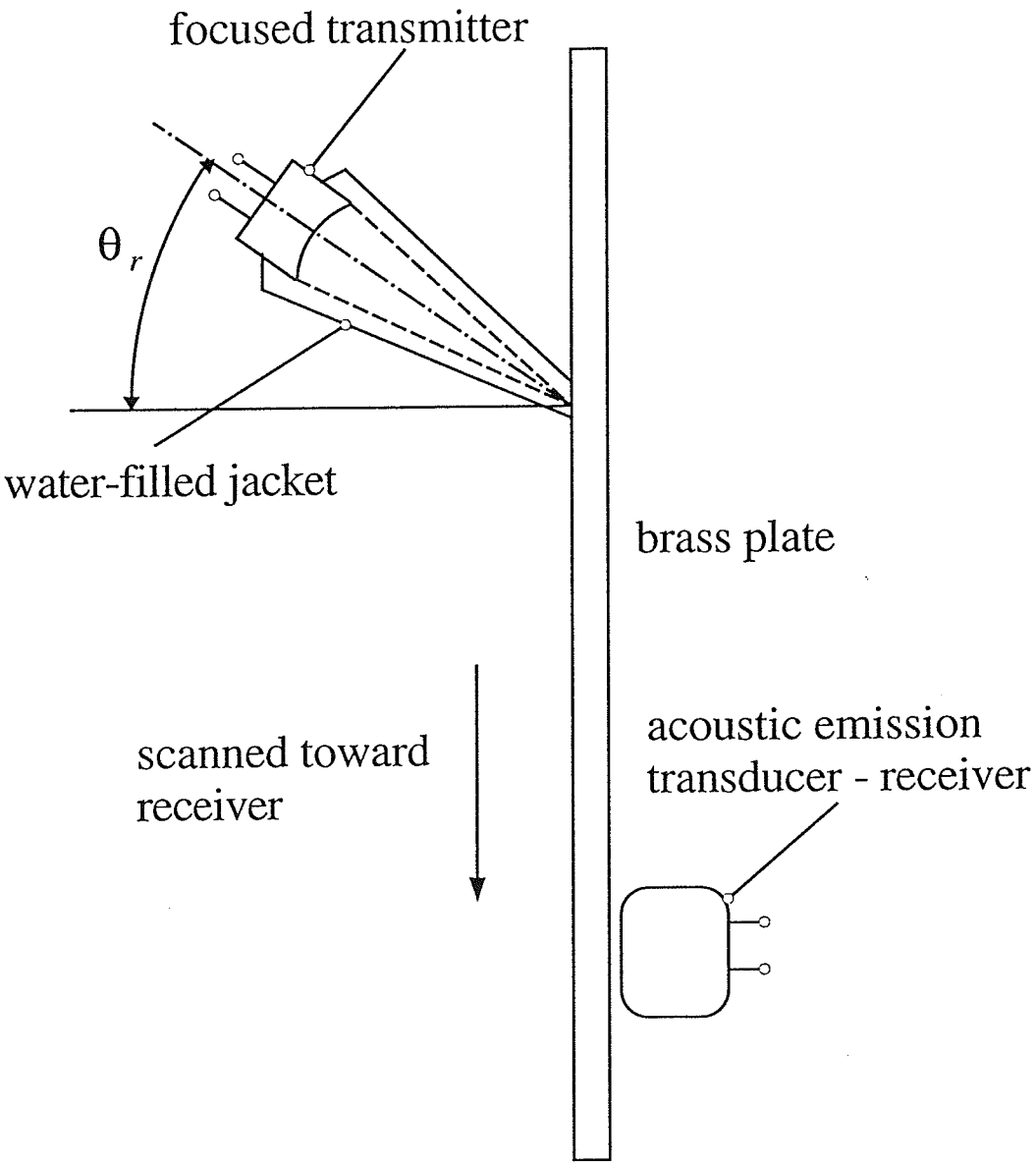

Figure 5. A sketch of the experimental arrangement viewed from the top. The central axis of the focused transducer makes an angle θ_r with the vertical. The sound is coupled to the plate by means of a water-filled jacket. The plate is otherwise loaded only by the surrounding air. The focal point is placed at the plate surface and moved toward the stationary receiving transducer.

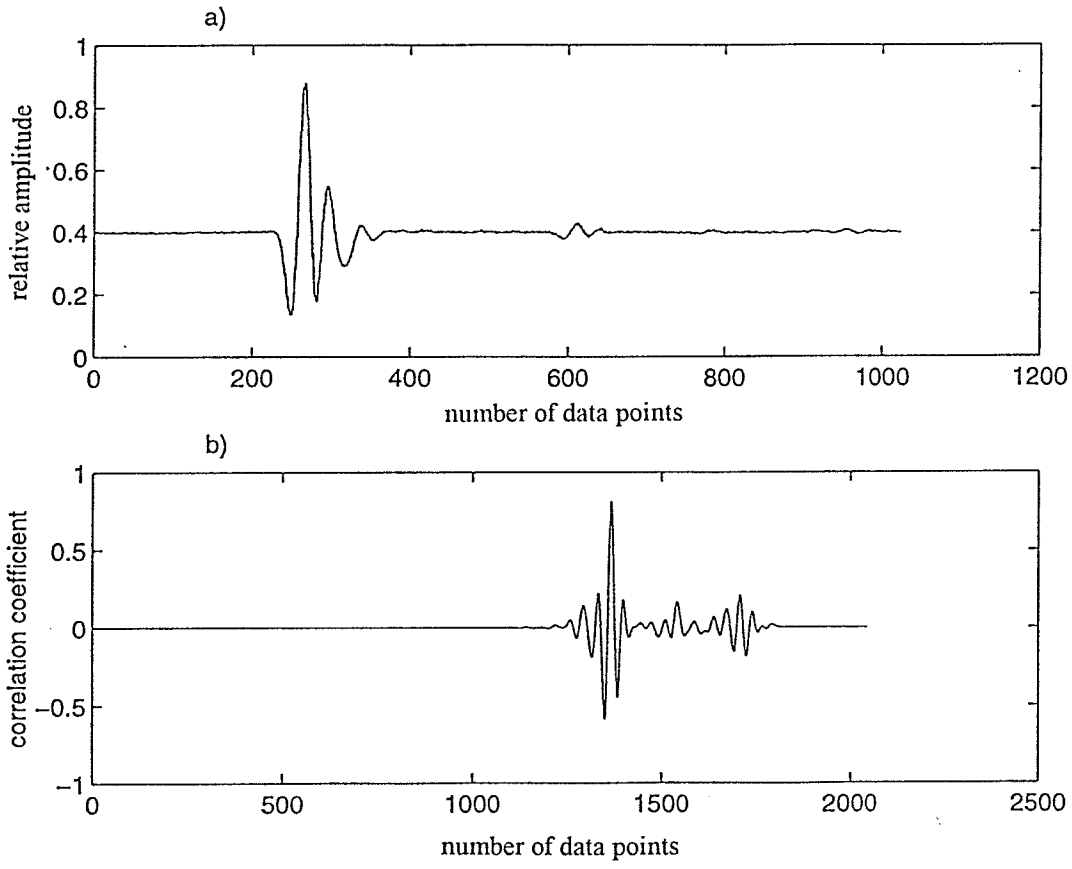

Figure 6. To calculate the longitudinal speed of sound in aluminum. (a) The length 1024 data record of the temporal, amplitude modulated, received signal. (b) The signal in (a) is broken into two signals, each of length 1024, T1 and T2. T1 has its first 512 data points set to zero and the next 512 data points identical to that of the signal in (a). The first 512 data points of T2 have the same values as their counterparts in the signal in (a) but have the next 512 data points set to zero. The correlation coefficient between the two signals, T1 and T2, is calculated and graphically presented.

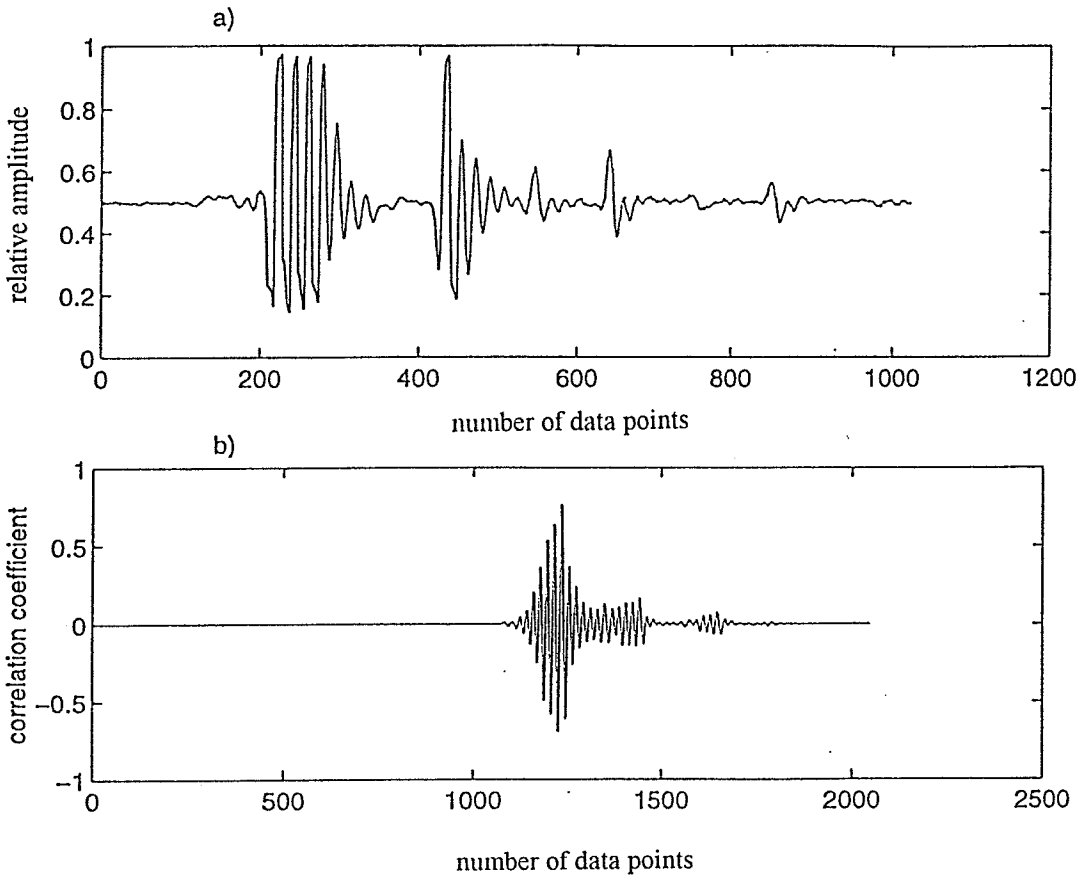

Figure 7. To calculate the longitudinal speed of sound in brass. (a) The length 1024 data record of the temporal, amplitude modulated, received signal. (b) The signal in (a) is broken into two signals, each of length 1024, T1 and T2. T1 has its first 400 data points set to zero and the next 624 data points identical to that of the signal in (a). The first 400 data points of T2 have the same values as their counterparts in the signal in (a) but have the next 624 data points set to zero. The correlation coefficient between the two signals, T1 and T2, is calculated and graphically presented.

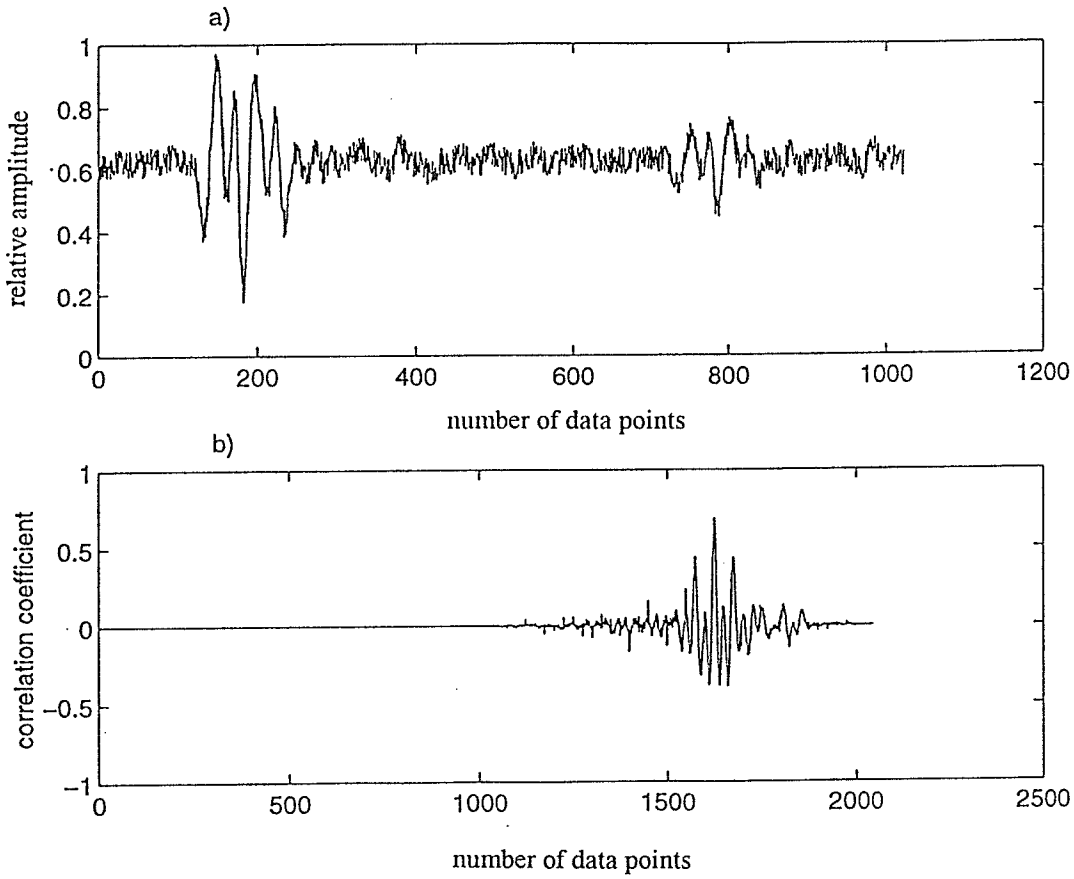

Figure 8. To calculate the longitudinal speed of sound in glass. (a) The length 1024 data record of the temporal, amplitude modulated, received signal. (b) The signal in (a) is broken into two signals, each of length 1024, T1 and T2. T1 has its first 512 data points set to zero and the next 512 data points identical to that of the signal in (a). The first 512 data points of T2 have the same values as their counterparts in the signal in (a) but have the next 512 data points set to zero. The correlation coefficient between the two signals, T1 and T2, is calculated and graphically presented.

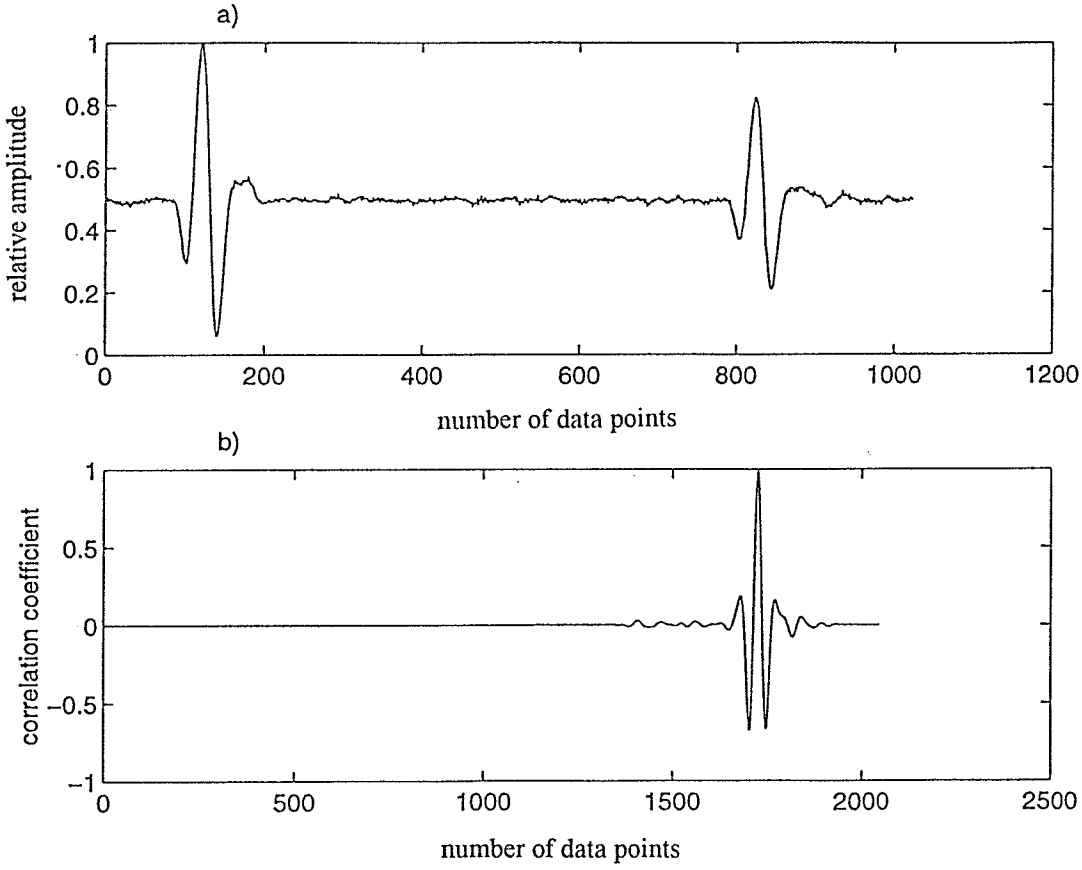

Figure 9. To calculate the shear speed of sound in aluminum. (a) The length 1024 data record of the temporal, amplitude modulated, received signal. (b) The signal in (a) is broken into two signals, each of length 1024, T1 and T2. T1 has its first 512 data points set to zero and the next 512 data points identical to that of the signal in (a). The first 512 data points of T2 have the same values as their counterparts in the signal in (a) but have the next 512 data points set to zero. The correlation coefficient between the two signals, T1 and T2, is calculated and graphically presented.

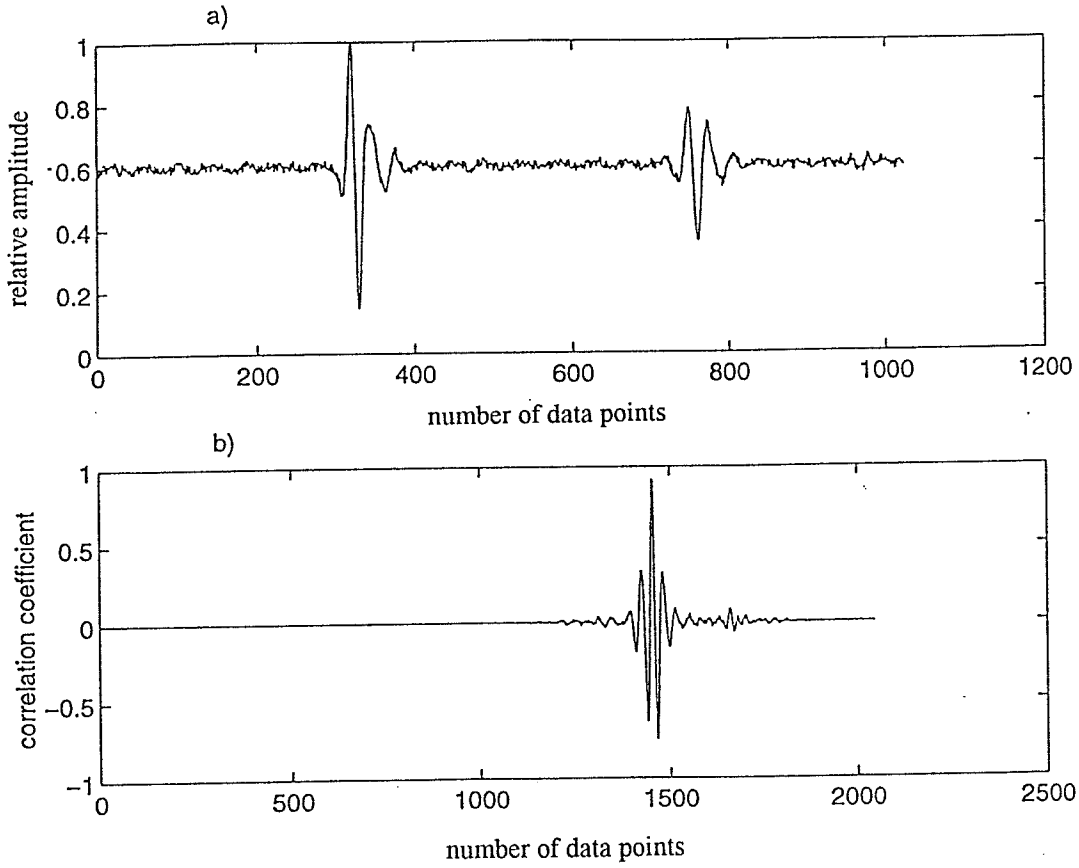

Figure 10. To calculate the shear speed of sound in brass. (a) The length 1024 data record of the temporal, amplitude modulated, received signal. (b) The signal in (a) is broken into two signals, each of length 1024, T1 and T2. T1 has its first 512 data points set to zero and the next 512 data points identical to that of the signal in (a). The first 512 data points of T2 have the same values as their counterparts in the signal in (a) but have the next 512 data points set to zero. The correlation coefficient between the two signals, T1 and T2, is calculated and graphically presented.

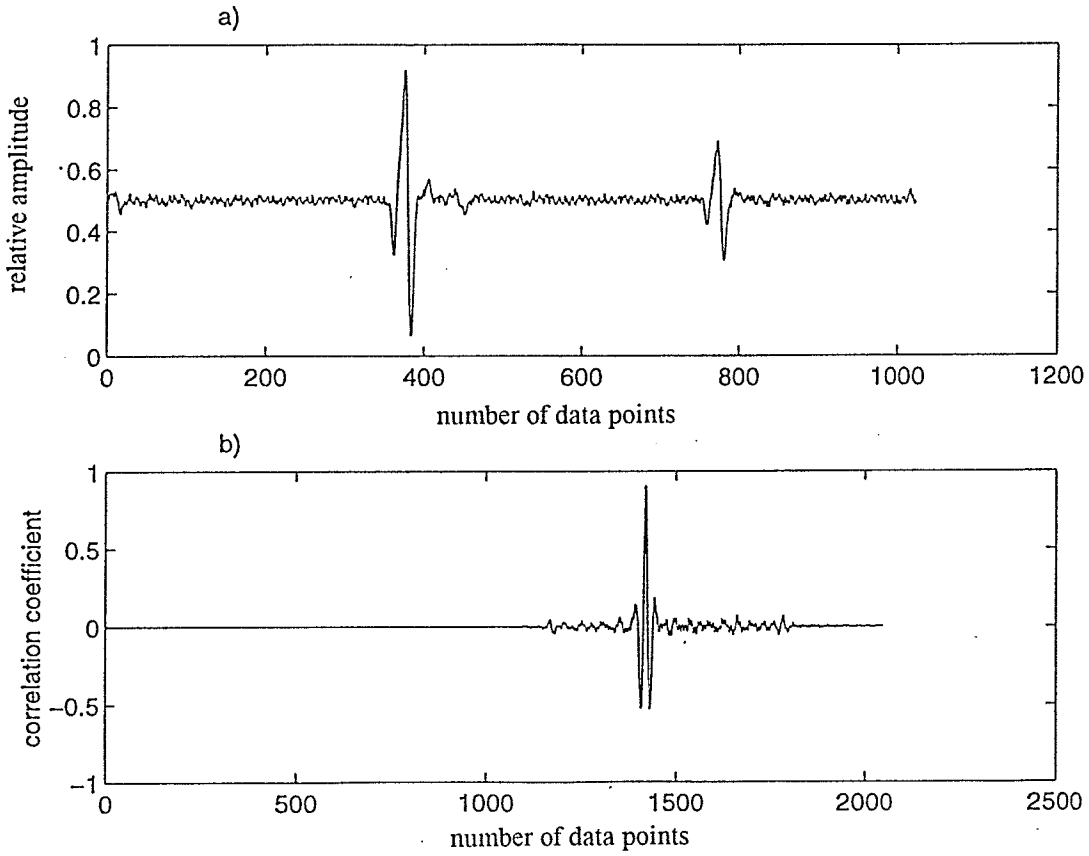

Figure 11. To calculate the shear speed of sound in glass. (a) The length 1024 data record of the temporal, amplitude modulated, received signal. (b) The signal in (a) is broken into two signals, each of length 1024, T1 and T2. T1 has its first 512 data points set to zero and the next 512 data points identical to that of the signal in (a). The first 512 data points of T2 have the same values as their counterparts in the signal in (a) but have the next 512 data points set to zero. The correlation coefficient between the two signals, T1 and T2, is calculated and graphically presented.

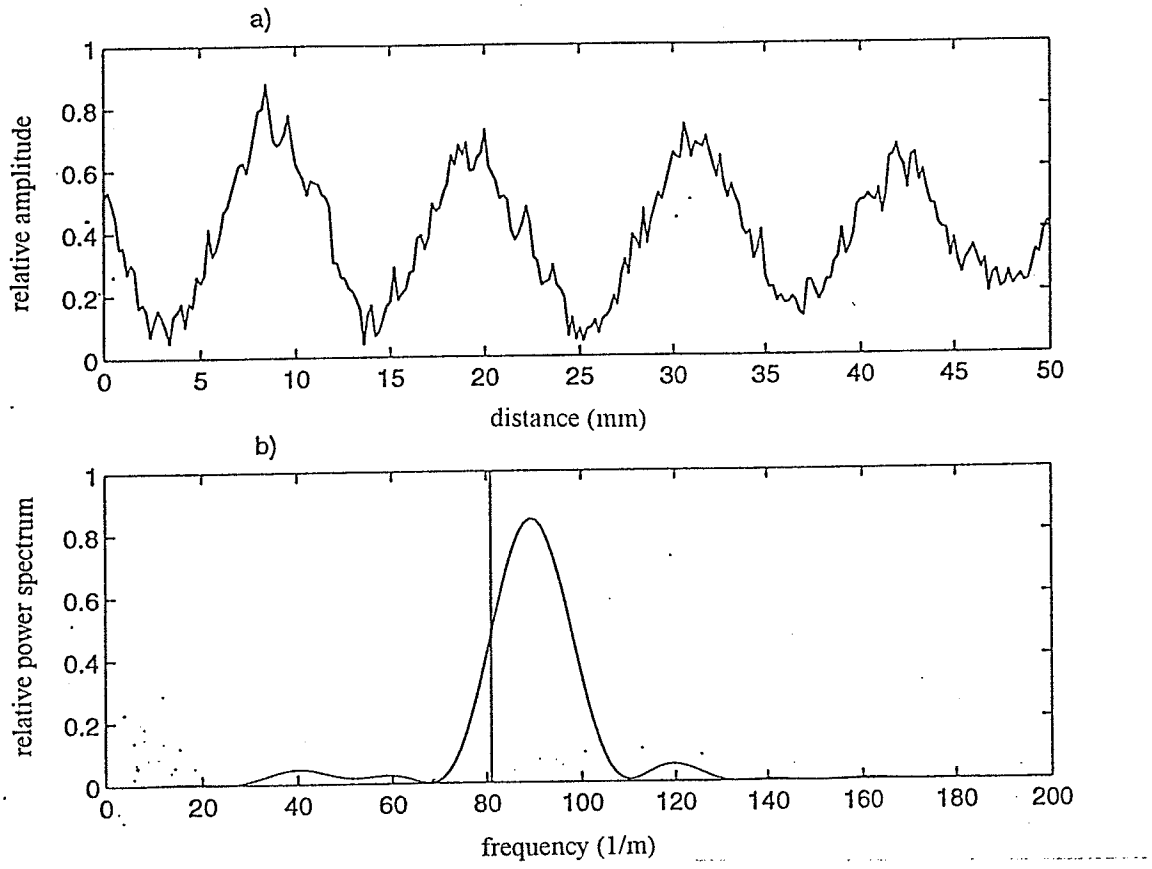

Figure 12. Representative data for aluminum, case 2 of Table 1. (a) The spatially, amplitude modulated, received signal plotted against position along the plate's surface (250 RMS data points, 50 *mm* scan distance). (b) The power spectrum of the signal from (a) plotted against the spatial frequency (1/distance). The vertical line indicates the theoretically estimated spatial beat frequency, $L = \pi c_t / (\varepsilon \omega)$.

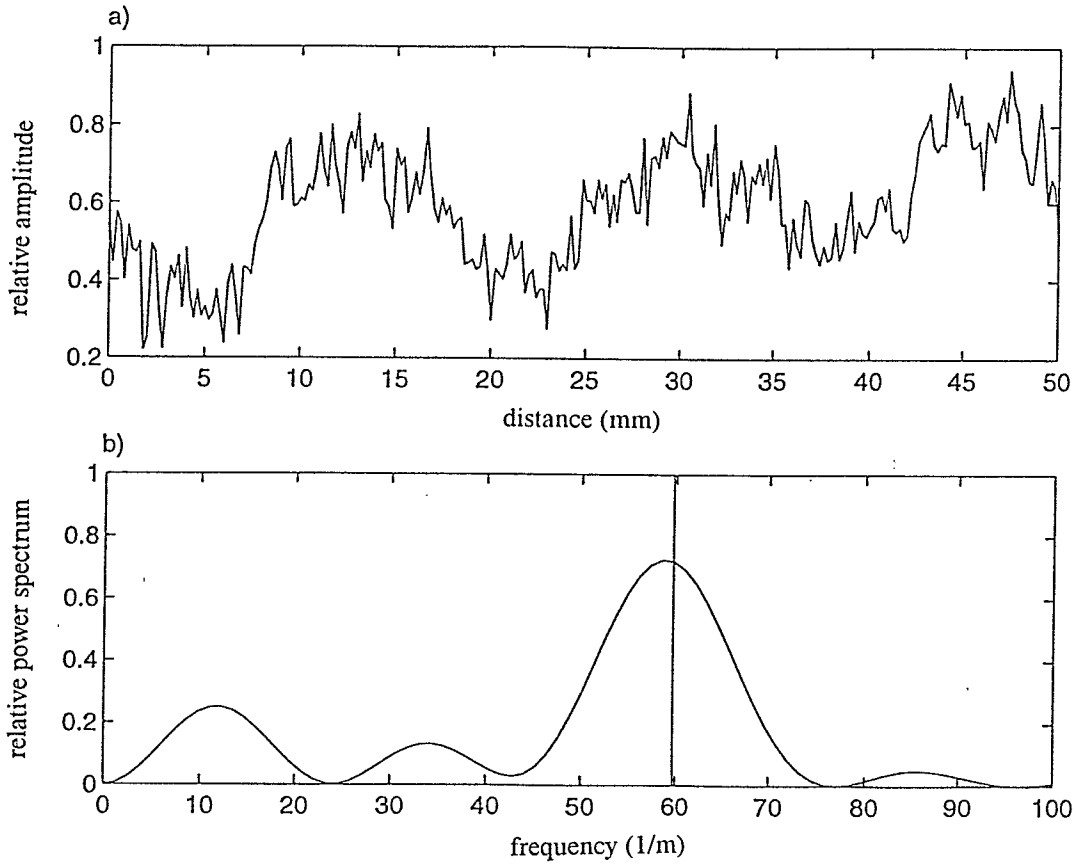

Figure 13. Representative data for brass, case 4 of Table 2. (a) The spatially, amplitude modulated, received signal plotted against position along the plate's surface (250 RMS data points, 50 *mm* scan distance). (b) The power spectrum of the signal from (a) plotted against the spatial frequency (1/distance). The vertical line indicates the theoretically estimated spatial beat frequency, $L = \pi c_t / (\varepsilon \omega)$.

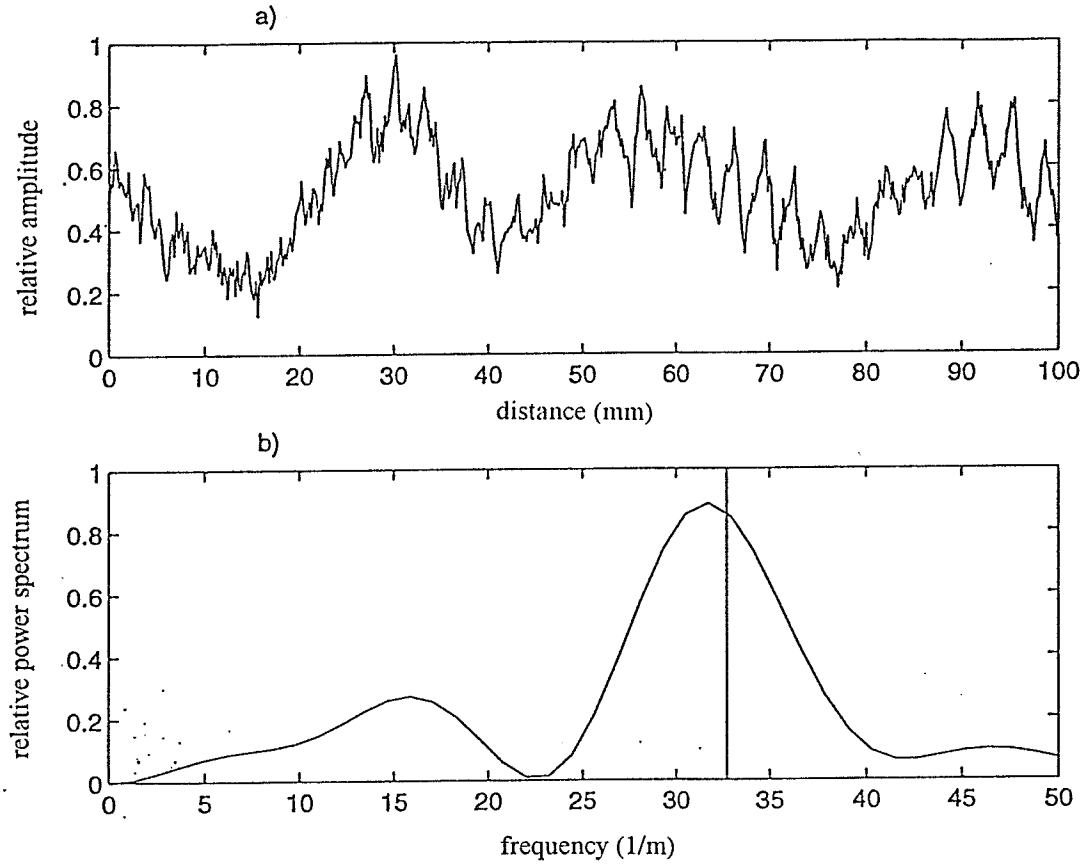

Figure 14. Representative data for glass, case 5 of Table 3. (a) The spatially, amplitude modulated, received signal plotted against position along the plate's surface (500 RMS data points, 100 *mm* scan distance). (b) The power spectrum of the signal from (a) plotted against the spatial frequency (1/distance). The vertical line indicates the theoretically estimated spatial beat frequency, $L = \pi c_t / (\varepsilon \omega)$.

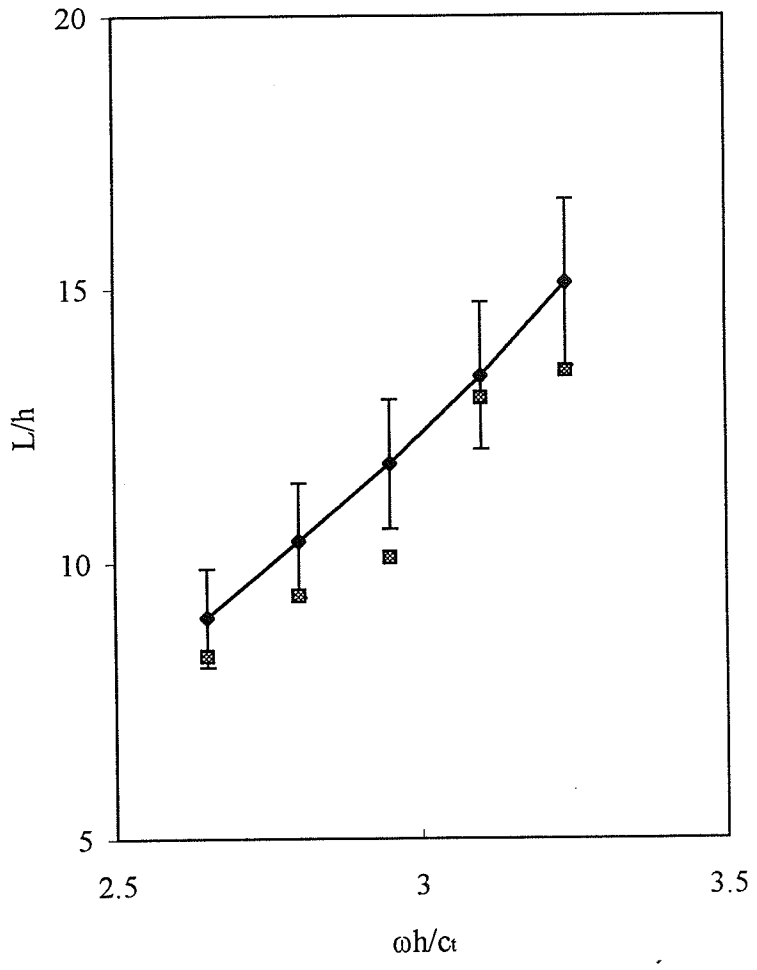

Figure 15. A plot of L/h against $\omega h / c_t$ for aluminum. The data points, represented by squares, are the measured results. The data points represented by diamonds are the theoretically predicted results. A ± 10% error bar is attached to each of the theoretically predicted results.

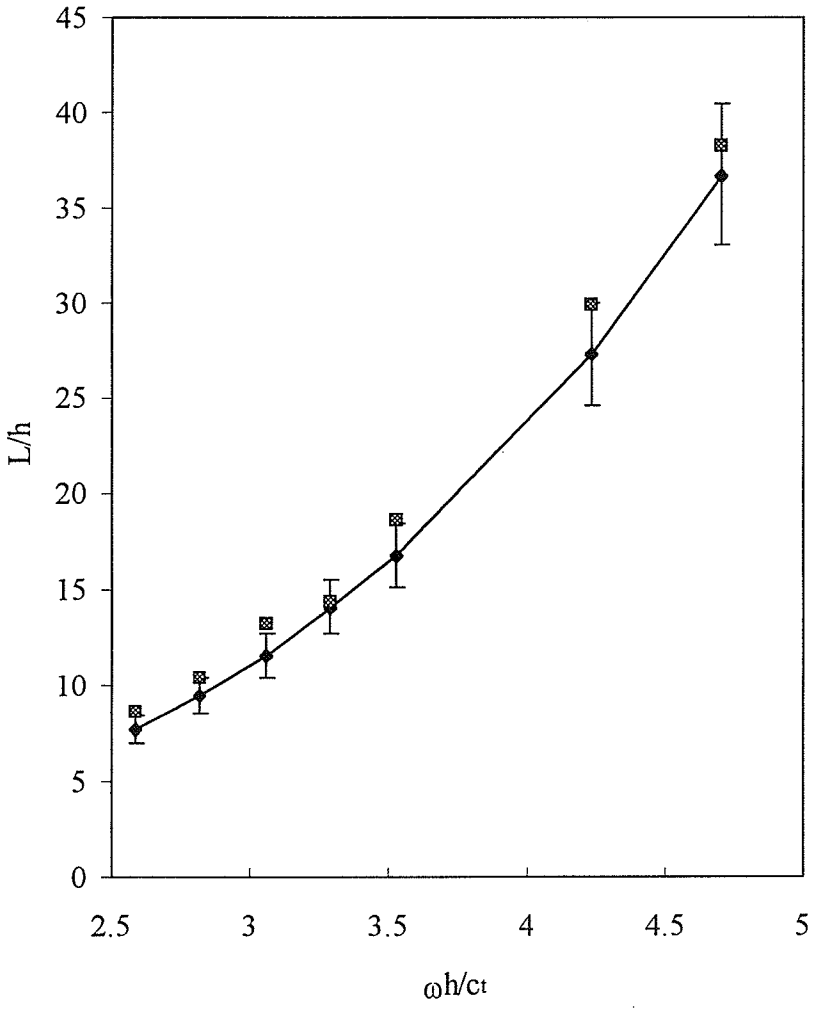

Figure 16. A plot of L/h against $\omega h / c_t$ for brass. The data points, represented by squares, are the measured results. The data points represented by diamonds are the theoretically predicted results. A ± 10% error bar is attached to each of the theoretically predicted results.

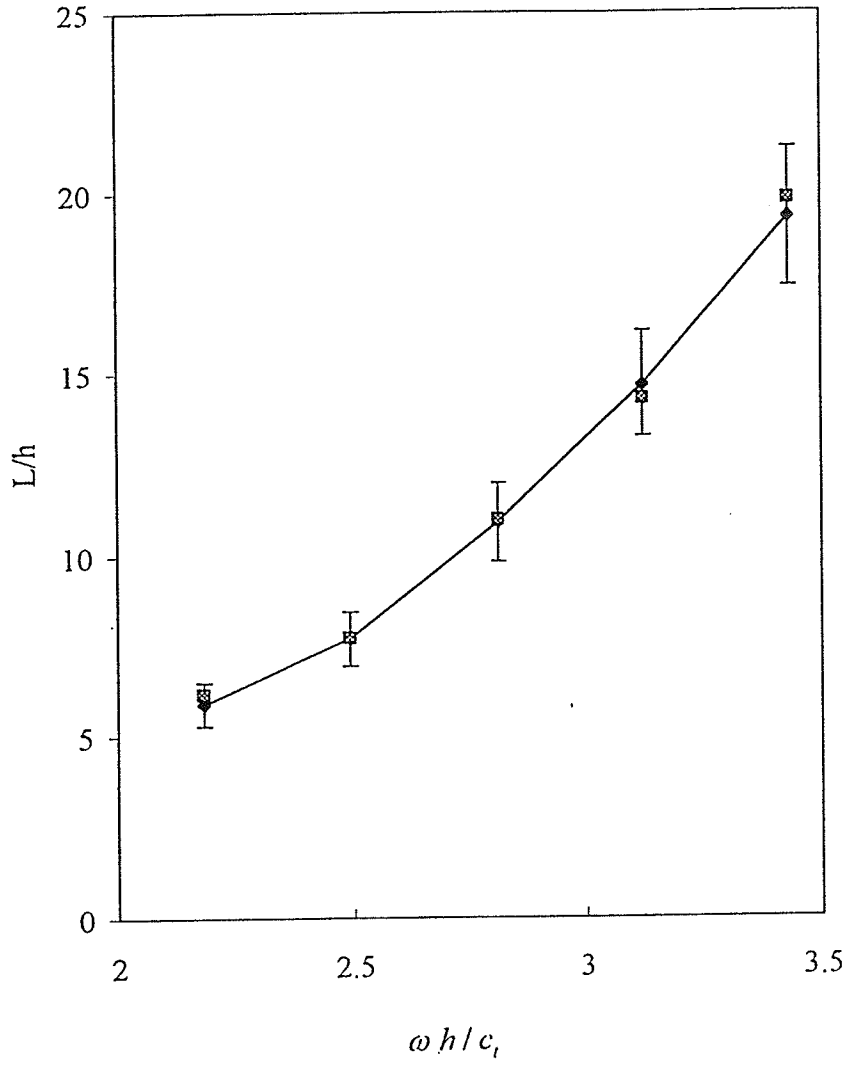

Figure 17. A plot of L/h against $\omega h / c_t$ for glass. The data points, represented by squares, are the measured results. The data points represented by diamonds are the theoretically predicted results. A ± 10% error bar is attached to each of the theoretically predicted results.

Table 1. The values of β_s, β_a, β_r, ε, β/ε, L, L/h and f_a were calculated for different transmit frequencies, f and $\omega h / c_t$ for a 2.38 *mm* aluminum plate. The Rayleigh angle, θ_r, and the Rayleigh speed, c_r, were also calculated using Eqs. (6) and (7).

Material	Aluminum		Thickness *(mm)*	2.38125
c_l *(m/s)*	6902		c_r *(m/s)*	3158
c_t *(m/s)*	3382		θ_r *(°)*	28.92

Case	*f (MHz)*	$\omega h / c_t$	β_s	β_a
1	1.20	2.65	0.863	1.125
2	1.26	2.80	0.903	1.119
3	1.33	2.95	0.934	1.114
4	1.4	3.10	0.959	1.110
5	1.46	3.24	0.978	1.106

Case	ε	β_r	β_r / ε	*L(mm)*
1	0.131	0.994	7.59	10.8
2	0.108	1.011	9.36	12.4
3	0.090	1.024	11.39	14.1
4	0.075	1.034	13.70	16.0
5	0.064	1.042	16.30	18.0

Case	*L/h*	f_a *(m^{-1})*
1	9.0	92.9
2	10.4	80.9
3	11.8	70.9
4	13.4	62.5
5	15.1	55.4

Table 2. The values of β_s, β_a, β_r, ε, β/ε, L, L/h and f_a were calculated for different transmit frequencies, f and $\omega h / c_t$ for a 2.38 *mm* brass plate. The Rayleigh angle, θ_r, and the Rayleigh speed, c_r, were calculated using Eqs. (6) and (7).

Material	Brass		Thickness *(mm)*	2.38125
c_l *(m/s)*	4536		c_r *(m/s)*	2069
c_t *(m/s)*	2215		θ_r $(^o)$	47.58

Case	*f (MHz)*	$\omega h / c_t$	β_s	β_a
1	0.73	2.59	0.802	1.133
2	0.80	2.82	0.877	1.123
3	0.86	3.06	0.930	1.115
4	0.93	3.29	0.966	1.108
5	1.00	3.53	0.991	1.102
6	1.20	4.23	1.033	1.090
7	1.33	4.70	1.047	1.085

Case	ε	β_r	β_r / ε	*L(mm)*
1	0.166	0.968	5.84	9.1
2	0.123	1.000	8.13	11.3
3	0.092	1.022	11.06	13.8
4	0.071	1.037	14.63	16.7
5	0.055	1.047	18.91	20.0
6	0.028	1.062	37.34	32.5
7	0.019	1.066	56.10	43.7

Case	*L/h*	f_a (m^{-1})
1	7.7	109.8
2	9.5	88.9
3	11.6	72.3
4	14.1	59.7
5	16.8	50.0
6	27.3	30.8
7	36.7	22.9

Table 3. The values of β_s, β_a, β_r, ε, β/ε, L, L/h and f_a were calculated for different transmit frequencies, f and $\omega h/c_t$ for a 3.18 *mm* glass plate. The Rayleigh angle, θ_r, and the Rayleigh speed, c_r, were also calculated using Eqs. (6) and (7).

Material	Glass		Thickness *(mm)*	3.175
c_l *(m/s)*	5257		c_r *(m/s)*	2920
c_t *(m/s)*	3199		θ_r *(°)*	31.53

Case	*f (MHz)*	$\omega h/c_t$	β_s	β_a
1	0.70	2.18	0.696	1.183
2	0.80	2.49	0.833	1.162
3	0.90	2.81	0.941	1.147
4	1.00	3.12	0.998	1.135
5	1.10	3.43	1.032	1.127

Case	ε	β_r	β_r/ε	*L(mm)*
1	0.243	0.939	3.86	9.39
2	0.164	0.998	6.07	12.2
3	0.103	1.044	10.15	17.3
4	0.069	1.067	15.57	23.3
5	0.048	1.079	22.68	30.6

Case	*L/h*	f_a *(m^{-1})*
1	5.9	106.5
2	7.7	82.2
3	10.9	57.9
4	14.7	42.9
5	19.3	32.7

Table 4. The measured and calculated values of L, L/h and f_a for different transmit frequencies, f and $\omega h / c_t$ for a 2.38 *mm* aluminum plate.

Material	Aluminum	Thickness *(mm)*	2.38125
c_l *(m/s)*	6902	c_r *(m/s)*	3158
c_t *(m/s)*	3382	θ_r $(^o)$	28.92

Case	f *(MHz)*	$\omega h / c_t$	β_r / ε
1	1.20	2.65	7.59
2	1.26	2.80	9.36
3	1.33	2.95	11.39
4	1.4	3.10	13.70
5	1.46	3.24	16.30

Theoretical Predictions

Case	*L(mm)*	*L/h*	f_a (m^{-1})
1	10.8	9.0	92.9
2	12.4	10.4	80.9
3	14.1	11.8	70.9
4	16.0	13.4	62.5
5	18.0	15.1	55.4

Measured Values

Case	*L(mm)*	*L/h*	f_a (m^{-1})
1	9.9	8.3	101.3
2	11.2	9.4	89.1
3	12.0	10.1	83.0
4	15.5	13.0	64.7
5	16.1	13.5	62.3

Table 5. The measured and calculated values of L, L/h and f_a for different transmit frequencies, f and $\omega h / c_t$ for a 2.38 *mm* brass plate.

Material	Brass	Thickness *(mm)*	2.38125
c_l *(m/s)*	4536	c_r *(m/s)*	2069
c_t *(m/s)*	2215	θ_r (^{o})	47.58

Case	f *(MHz)*	$\omega h / c_t$	β_r / ε
1	0.73	2.59	5.84
2	0.80	2.82	8.13
3	0.86	3.06	11.06
4	0.93	3.29	14.63
5	1.00	3.53	18.91
6	1.20	4.23	37.34
7	1.33	4.70	56.10

Theoretical Predictions

Case	*L(mm)*	*L/h*	f_a (m^{-1})
1	9.1	7.7	109.8
2	11.3	9.5	88.9
3	13.8	11.6	72.3
4	16.7	14.1	59.7
5	20.0	16.8	50.0
6	32.5	27.3	30.8
7	43.7	36.7	22.9

Measured Values

Case	*L(mm)*	*L/h*	f_a (m^{-1})
1	10.2	8.6	97.7
2	12.4	10.4	80.6
3	15.7	13.2	63.5
4	17.1	14.4	58.6
5	22.1	18.6	45.2
6	35.6	29.9	28.1
7	45.5	38.2	22.0

Table 6. The measured and calculated values of L, L/h and f_a for different transmit frequencies, f and $\omega h / c_t$ for a 3.18 *mm* glass plate.

Material	Glass	Thickness *(mm)*	3.175
c_l *(m/s)*	5257	c_r *(m/s)*	2920
c_t *(m/s)*	3199	θ_r $(^o)$	31.53

Case	f *(MHz)*	$\omega h / c_t$	β_r / ε
1	0.70	2.18	3.86
2	0.80	2.49	6.07
3	0.90	2.81	10.15
4	1.00	3.12	15.57
5	1.10	3.43	22.68

Theoretical Predictions

Case	*L(mm)*	*L/h*	f_a (m^{-1})
1	9.39	5.9	106.5
2	12.2	7.7	82.2
3	17.3	10.9	57.9
4	23.3	14.7	42.9
5	30.6	19.3	32.7

Measured Values

Case	*L(mm)*	*L/h*	f_a (m^{-1})
1	9.9	6.2	101.3
2	12.2	7.7	81.8
3	17.4	11.0	57.4
4	22.7	14.3	44.0
5	31.5	19.8	31.7

Table 7. An assessment of the accuracy of the longitudinal and shear speeds in the various elastic plates. The following variables are tabulated: the round-trip time taken from one face of the elastic plate to the other and back to the first face of the elastic plate, t; the thickness of the plate, $2h$; the longitudinal or shear speed in the various elastic plates, c, calculated using Eq. (3); and Δc; which is calculated using Eq. (9).

Material	2h (mm)	Δ2h (mm)	t (ns)	Δt (ns)	Speed	c (m/s)	Δc (m/s)	Δc (%)
Aluminum	2.381	0.141	690	2	c_l	6902	429	6.2
Aluminum	2.381	0.141	1408	2	c_t	3382	205	6.1
Brass	2.381	0.121	1050	5	c_l	4536	252	5.6
Brass	2.381	0.121	2150	5	c_t	2215	118	5.3
Glass	3.175	0.054	1208	2	c_l	5257	98	1.9
Glass	3.175	0.054	1985	2	c_t	3199	58	1.8

APPENDIX A DERIVATION OF BEATLENGTH

A.1 Introduction

Assuming a thin, isotropic and homogeneous elastic plate with infinite planar dimensions, an acoustic surface wave beating phenomenon can be observed with an ultrasound beam impacting the aforementioned plate at the Rayleigh angle. The derivation for the beatlength from first principles follows.

A.2 Terms and Definitions

Let the plane of the elastic plate be defined by the x_1- and x_2-axes and the center of the elastic plate be $x_3 = 0$. The top and bottom surfaces of the elastic plate are defined as being at $x_3=h$ and $x_3=-h$, respectively.

The following is a partial list of symbols. When appropriate, defining equations and relationships are introduced.

f	frequency
$\omega = 2\,\pi f$	angular frequency
c_l	longitudinal wave speed
c_t	transverse or shear wave speed
$k = \frac{\omega}{c_l}$	longitudinal wave number
$\mathcal{H} = \frac{\omega}{c_t}$	transverse wave number
ξ	projection of the longitudinal wave number onto the x_1-axis. Also the projection of the transverse wave number onto the x_1-axis

$\beta = \frac{\xi}{\mathcal{H}}$ normalized wave number

$\kappa = \frac{k}{\mathcal{H}} = \frac{c_t}{c_l}$ ratio of the transverse speed over the longitudinal speed

$k_3 = \sqrt{k^2 - \xi^2} = \mathcal{H}\sqrt{\kappa^2 - \beta^2} = \mathcal{H}\,\gamma_l$

projection of the longitudinal wave number onto the x_3-axis

$\gamma_l = \sqrt{\kappa^2 - \beta^2}$

$\mathcal{H}_3 = \sqrt{\mathcal{H}^2 - \xi^2} = \mathcal{H}\sqrt{1 - \beta^2} = \mathcal{H}\,\gamma_t$

projection of the transverse wave number onto the x_3-axis

$\gamma_t = \sqrt{1 - \beta^2}$

$\sigma_l = k_3\, h = \mathcal{H}\,\gamma_l h$

$\sigma_t = \mathcal{H}_3\, h = \mathcal{H}\,\gamma_t h$

$$p = \frac{\xi^2 - \frac{\mathcal{H}^2}{2}}{\xi} = \frac{\mathcal{H}\,(\beta^2 - \frac{1}{2})}{\beta} = \mathcal{H}\,\rho$$

$$\rho = \frac{(\beta^2 - \frac{1}{2})}{\beta}$$

A.3 Scalar and Vector Potentials

Assume guided acoustic waves are launched along the x_1-direction by a wave incident at an angle with the normal to the plate equal to the Rayleigh angle. Standing-wave patterns will be set up along the x_3-direction while a traveling wave will propagate along the x_1-direction. The scalar and vector potentials can be written as follows :

$$\varphi = \left[C_1 \cos(k_3 x_3) + C_2 \sin(k_3 x_3)\right] e^{i(\xi x_1 - ct)}$$

$$= \left[C_1 \cos(k_3 h \underline{x}_3) + C_2 \sin(k_3 h \underline{x}_3)\right] e^{i(\xi x_1 - ct)} \quad \text{(A.1)}$$

$$\Psi = \left[D_1 \cos(\mathcal{H}_3 x_3) + D_2 \sin(\mathcal{H}_3 x_3)\right] e^{i(\xi x_1 - ct)}$$

$$= \left[D_1 \cos(\mathcal{H}_3 h \underline{x}_3) + D_2 \sin(\mathcal{H}_3 h \underline{x}_3)\right] e^{i(\xi x_1 - ct)} \quad \text{(A.2)}$$

A.4 Displacement Equations

The term u_i is the displacement amplitude of the surface wave on the plate traveling along the x_i-direction. The acoustic beam is assumed to impact the plate in the x_1- x_3 plane making an angle of incidence equal to the Rayleigh angle.

$$u_1 = \frac{\partial \varphi}{\partial x_1} - \frac{\partial \Psi}{\partial x_3} \quad \text{(A.3)}$$

$$u_3 = \frac{\partial \varphi}{\partial x_3} + \frac{\partial \Psi}{\partial x_1} \quad \text{(A.4)}$$

A.5 Boundary Conditions

The boundary conditions on the plate for free waves are as follows.

At $x_3 = \pm h$, the stresses on the surface of the plate are given by

$$T_{31} = T_{32} = T_{33} = 0 \quad \text{(A.5)}$$

where T_{ij} is the component of the stress in the j-direction on a plane perpendicular to the i-axis. The generalized Hooke's Law for an isotropic body is given by

$$T_{ij} = \lambda \sum \mathrm{e}_{kk} \delta_{ij} + 2\mu e_{ij} \quad \text{(A.6)}$$

where e_{ij} is the strain tensor component in the j-direction on a plane perpendicular to the i-axis. For small strains,

$$e_{ij} = \frac{1}{2}\left(\frac{\partial u_i}{\partial x_j} + \frac{\partial u_j}{\partial x_i}\right) \tag{A.7}$$

A.6 Symmetric Wave Displacements

The potentials are

$$\varphi = \left[C_1 \cos(k_3 x_3) + C_2 \sin(k_3 x_3)\right] e^{i(\xi x_1 - ct)} \tag{A.8}$$

$$\Psi = \left[D_1 \cos(\mathcal{H}_3 x_3) + D_2 \sin(\mathcal{H}_3 x_3)\right] e^{i(\xi x_1 - ct)} \tag{A.9}$$

The corresponding particle displacements are

$$u_{1s} = \left[i\xi C_1 \cos(k_3 x_3) - \mathcal{H}_3 D_2 \cos(\mathcal{H}_3 x_3)\right] e^{i(\xi x_1 - ct)} \tag{A.10}$$

$$u_{3s} = \left[-C_1 k_3 \sin(k_3 x_3) + i\xi D_2 \sin(\mathcal{H}_3 x_3)\right] e^{i(\xi x_1 - ct)} \tag{A.11}$$

At $x_3 = \pm h$,

$$iC_1 \sigma_L \sin(k_3 x_3) + phD_2 \sin(\mathcal{H}_3 x_3) = 0 \tag{A.12}$$

$$phC_1 \cos(\sigma_l) + i\sigma_t D_2 \cos(\sigma_t) = 0 \tag{A.13}$$

The dispersion relation is found by demanding a non-trivial solution for the two equations. The vanishing determinant gives

$$\sigma_l \sigma_t \tan(\sigma_l) + (ph)^2 \tan(\sigma_t) = 0 \tag{A.14}$$

which can be rewritten as

$$\gamma_l \gamma_t \tan(\mathcal{H} h \gamma_l) + \rho^2 \tan(\mathcal{H} h \gamma_t) = 0 \tag{A.15}$$

The x_1-displacement becomes

$$u_{1s} = C_S\left[\frac{\cosh(\mathcal{H}h|\gamma_l|\underline{x}_3)}{\cosh(\mathcal{H}h|\gamma_l|)} - \left(1-\frac{1}{2\beta^2}\right)\frac{\cosh(\mathcal{H}\,\mathrm{h}|\gamma_t|\underline{x}_3)}{\cosh(\mathcal{H}h|\gamma_t|)}\right]e^{i\left(\frac{\omega\beta}{c_t}x_1 - ct\right)} \tag{A.16}$$

where $C_s = i\xi C_1\cosh(|\sigma_l|)$

Similarly, the x_3-displacement becomes

$$u_{3s} = \frac{-iC_s|\gamma_l|}{\beta}\left[\frac{\sinh(\mathcal{H}\,\mathrm{h}|\gamma_l|\underline{x}_3)}{\cosh(\mathcal{H}\,\mathrm{h}|\gamma_l|)} - \frac{\left(\beta^2-\frac{1}{2}\right)\sinh(\mathcal{H}\,\mathrm{h}|\gamma_t|\underline{x}_3)}{|\gamma_l||\gamma_t|\cosh(\mathcal{H}\,\mathrm{h}|\gamma_t|)}\right]e^{i\left(\frac{\omega\beta}{c_t}x_1 - ct\right)} \tag{A.17}$$

A.7 Brekhovskikh's and Goncharov's Estimate

Starting from the dispersion relation:

$$\gamma_l\gamma_t\tan(\mathcal{H}h\gamma_l) + \rho^2\tan(\mathcal{H}h\gamma_t) = 0 \tag{A.18}$$

Assuming that $|\mathcal{H}h\gamma_l|$ and $|\mathcal{H}h\gamma_t|$ are large,

$$\tan(\mathcal{H}h\gamma_l) = i\tanh(\mathcal{H}h|\gamma_l|) \approx i\left(1-2e^{-2\mathcal{H}h|\gamma_l|}\right) \tag{A.19}$$

$$\tan(\mathcal{H}h\gamma_t) = i\tanh(\mathcal{H}h|\gamma_t|) \approx i\left(1-2e^{-2\mathcal{H}h|\gamma_t|}\right) \tag{A.20}$$

After substituting into the dispersion relation:

$$\gamma_l\gamma_t\left(1-2e^{-2\mathcal{H}h|\gamma_l|}\right) + \rho^2\left(1-2e^{-2\mathcal{H}h|\gamma_t|}\right) = 0 \tag{A.21}$$

Let $$f(\beta) = \gamma_l\gamma_t + \rho^2 = 2\gamma_l\gamma_t e^{-2\mathcal{H}h|\gamma_l|} + \rho^2 2e^{-2\mathcal{H}h|\gamma_t|} \tag{A.22}$$

$$\mathrm{f_r}(\beta) \approx (\beta-\beta_\mathrm{r})\mathrm{f_r'}(\beta_\mathrm{r}) \tag{A.23}$$

where $$f_r'(\beta) = \frac{-\beta\sqrt{\kappa^2-\beta^2}}{\sqrt{1-\beta^2}} - \frac{\beta\sqrt{1-\beta^2}}{\sqrt{\kappa^2-\beta^2}} + 2\beta - \frac{1}{2\beta^3} \tag{A.24}$$

Setting $\beta_s = \beta_r - \varepsilon$

$$\varepsilon \approx -2\left\{\frac{\rho^2\left[e^{-2\mathcal{H}h|\gamma_t|} - e^{-2\mathcal{H}h|\gamma_l|}\right]}{\left[f_r'(\beta)\right]}\right\}_{\beta=\beta_r} \tag{A.25}$$

The particle can now be approximated as

$$u_{1s} = C_S\left[\frac{\cosh(\mathcal{H}h|\gamma_l|\underline{x}_3)}{\cosh(\mathcal{H}h|\gamma_l|)} - \left(1 - \frac{1}{2\beta_r^{\,2}}\right)\frac{\cosh(\mathcal{H}\,\mathrm{h}|\gamma_t|\underline{x}_3)}{\cosh(\mathcal{H}h|\gamma_t|)}\right]e^{i\left(\frac{\omega}{c_t}(\beta_r-\varepsilon)x_1 - ct\right)} \tag{A.26}$$

$$u_{3s} = \frac{-iC_s|\gamma_l|}{\beta_r}\left[\frac{\sinh(\mathcal{H}\,\mathrm{h}|\gamma_l|\underline{x}_3)}{\cosh(\mathcal{H}\,\mathrm{h}|\gamma_l|)} - \frac{\left(\beta_r^2 - \frac{1}{2}\right)\sinh(\mathcal{H}\,\mathrm{h}|\gamma_t|\underline{x}_3)}{|\gamma_l|\|\gamma_t|\cosh(\mathcal{H}\,\mathrm{h}|\gamma_t|)}\right]e^{i\left(\frac{\omega}{c_t}(\beta_r-\varepsilon)x_1 - ct\right)} \tag{A.27}$$

A.8 Asymmetric Wave Displacements

The potentials are

$$\varphi = \left[C_1\cos(k_3x_3) + C_2\sin(k_3x_3)\right]e^{i(\xi x_1 - ct)} \tag{A.28}$$

$$\Psi = \left[D_1\cos(\mathcal{H}_3x_3) + D_2\sin(\mathcal{H}_3x_3)\right]e^{i(\xi x_1 - ct)} \tag{A.29}$$

Proceeding just as we did for the symmetric case, the dispersion relation is found to be

$$\gamma_l\gamma_t\tan(\mathcal{H}h\gamma_t) + \rho^2\tan(\mathcal{H}h\gamma_l) = 0 \tag{A.30}$$

Setting $\beta_a = \beta_r + \varepsilon$, the x_1-displacement becomes

$$u_{1a} = C_a\left[\frac{\sinh(\mathcal{H}h|\gamma_l|\underline{x}_3)}{\cosh(\mathcal{H}h|\gamma_l|)} - \left(1 - \frac{1}{2\beta^2}\right)\frac{\sinh(\mathcal{H}\,\mathrm{h}|\gamma_l|\underline{x}_3)}{\cosh(\mathcal{H}h|\gamma_l|)}\right]e^{i\left(\frac{\omega\beta}{c_t}x_1 - ct\right)} \tag{A.31}$$

Similarly, the x_3-displacement becomes

$$u_{3a} = -iC_a \frac{|\gamma_l|}{\beta}\left[\frac{\cosh(\mathcal{H}h|\gamma_l|\underline{x}_3)}{\cosh(\mathcal{H}h|\gamma_l|)} - \frac{1}{\left(1-\frac{1}{2\beta^2}\right)}\frac{\cosh(\mathcal{H}h|\gamma_t|\underline{x}_3)}{\cosh(\mathcal{H}h|\gamma_t|)}\right] e^{i\left(\frac{\omega\beta}{c_t}x_1 - ct\right)} \qquad \text{(A.32)}$$

Moreover,

$$u_{1a} = C_a\left[\frac{\sinh(\mathcal{H}h|\gamma_l|\underline{x}_3)}{\cosh(\mathcal{H}h|\gamma_l|)} - \left(1-\frac{1}{2\beta_r^{\,2}}\right)\frac{\sinh(\mathcal{H}h|\gamma_l|\underline{x}_3)}{\cosh(\mathcal{H}h|\gamma_l|)}\right] e^{i\left(\frac{\omega(\beta_r+\varepsilon)}{c_t}x_1 - ct\right)} \qquad \text{(A.33)}$$

and

$$u_{3a} = -iC_a \frac{|\gamma_l|}{\beta_r}\left[\frac{\cosh(\mathcal{H}h|\gamma_l|\underline{x}_3)}{\cosh(\mathcal{H}h|\gamma_l|)} - \frac{1}{\left(1-\frac{1}{2\beta_r^{\,2}}\right)}\frac{\cosh(\mathcal{H}h|\gamma_t|\underline{x}_3)}{\cosh(\mathcal{H}h|\gamma_t|)}\right] e^{i\left(\frac{\omega(\beta_r+\varepsilon)}{c_t}x_1 - ct\right)} \qquad \text{(A.34)}$$

By forming the sums $u_{1r} = u_{1s} + u_a$ and $u_{3r} = u_{3s} + u_{3a}$, we arrive at the approximate Rayleigh wave displacements sketched in Fig. 2.

A.9 Beatlength

The beat length is determined from the exponential terms of the displacements. The displacement equations can be written as

$$u_{1s} = C_s A_{1s}(x_3)\exp(i\mathcal{H}\beta_r x_1)\exp(-i\mathcal{H}\varepsilon x_1) \qquad \text{(A.35)}$$

$$u_{1a} = C_a B_{1s}(x_3)\exp(i\mathcal{H}\beta_r x_1)\exp(i\mathcal{H}\varepsilon x_1) \qquad \text{(A.36)}$$

so that $u_{1r} = u_{1s} + u_a$

$$= C\exp(i\mathcal{H}\beta_r x_1)\exp(-i\mathcal{H}\varepsilon x_1)\left[A_{1s}(x_3) + B_{1s}(x_3)\exp(2i\mathcal{H}\varepsilon x_1)\right] \qquad \text{(A.37)}$$

The expression for u_{3r} is similar.

There are two exponential terms in this expression:

$\exp(i\mathcal{H}\beta_r x_1)$ which varies with $L_p = \frac{2\pi}{\mathcal{H}\beta_r}$

and $\exp(2i\mathcal{H}\varepsilon x_1)$ which varies with $L_a = \frac{\pi}{\mathcal{H}\varepsilon}$

Because $\beta_r \rangle\rangle \varepsilon_\beta$, $L_a \gg L_p$

The beatlength L is L_a.

$$L = \frac{\pi}{\mathcal{H}\varepsilon} \tag{A.38}$$

APPENDIX B COMPUTER PROGRAMS

Program B.1. Sym.ma

This *Mathematica* program takes the transmit angular frequency, w, the longitudinal speed of sound , cl, the shear speed of sound, ct, the half-thickness, h, as inputs and solves two transcendental Lamb dispersion equations. There are three outputs, the first beta output is β_s, the second beta output is β_a, the third output is the ratio of the shear speed over the longitudinal speed. This is the trivial case solution to the transcendental equation.

```
ClearAll[w,kappa,cl,ct,k,h,f,g,beta];

kappa = ct/cl;

H = w/ct;

w=0.93e6*2*Pi;

cl=4536;

ct=2215;

h = (0.00238125)/2;

f = Sqrt[(1-beta^2)] Sqrt[(kappa^2-beta^2) ] Tan[ H h Sqrt[kappa^2-beta^2]] + ((beta^2-

0.5)/beta)^2 Tan[H h Sqrt[1-beta^2]];

NumberForm[FindRoot[f==0,{beta,3},MaxIterations ->50],10]

g = Sqrt[(1-beta^2)]Sqrt[ (kappa^2-beta^2) ] Tan[ H h Sqrt[1-beta^2]] + ((beta^2-

0.5)/beta)^2 Tan[H h Sqrt[kappa^2-beta^2]];

NumberForm[FindRoot[g==0,{beta,2.25},MaxIterations ->50],10]

NumberForm[N[kappa],10]
```

Program B.2. Rowscan.c

This C program is a data acquisition program resident in a 486 PC that interfaces with the Tektronix 11401 Oscilloscope and captures the screen data. This was written by Kay Raum and used with permission. When run, this program will prompt the user to supply the following information, *filename, scan axis(1 or 2 or 3), stepsize(in μm) and length of scan row(in mm).* Two output files will be generated, a binary file with *filename.bin* , which contains the unscaled integer signal points (1024 for each scan) and an ASCII file *filename.dat*, which contains waveform and scan information.

```
/*
| This program is written by Kay Raum                                    |
| I used some good ideas from Nadine B. Smith and Kate Hillsley.         |
| It is written to create a set of A-scan lines along one axis.          |
| The distance between two A-scan lines (stepsize) and the total         |
| length of a scan row is selectable as well as the axis of the          |
| Daedal system, which is used. The direction of the scan                |
| is always in the positive axis direction. You have to select the       |
| trace of the signal, which you want to grab from the Tektronix         |
| scope, too.                                                            |
| You should take care, that the scope is running in enhanced mode,      |
| otherwise scan information will not stored correctly.                  |
| Two files will be created. A binary file with extension .bin           |
| contains the unscaled integer signal points (1024 for each scan).      |
| The second file is an ASCII file, which contains waveform and scan     |
| information. You have to transfer the files separately in binary       |
| or ascii mode, respectively. To read the files in matlab, you          |
| should use my function file.m                                          |
|                                                                        |
| For questions and suggestions, send an e-mail to                       |
|  raum@uibrl.brl.uiuc.edu                                               |
|                                                                        |
^^^^^^^^^^^^^^^^^^^^^^^^^^^^^^^^^^^^^^^^^^^^^^^^^^^^^^^^^^^^^^^^^^^^^^^^ */

#include <conio.h>
#include <stdio.h>
#include <string.h>
#include <stdlib.h>
#include "c:\qc2\include\msgraph.h"
#include <time.h>
#include "c:\at-gpib\c\decl.h"

#define ERR    (1<<15)     /* Error detected          */
#define TIMO   (1<<14)     /* Timeout                 */
#define RQS    (1<<11)     /* Device needs service    */
```

```
void introduction(void);
void init_parameter(void);
void init_files(void);
void init_device(void);
void measure(void);
void disable_device(void);

FILE
        *fopen(),
        *ptr_dat,
        *ptr_bin;

char filebin[25],
        filedat[25],
        command[30],
        wait[20],
        wfm[250],
        op,
        asr[4];

char ax_number;

unsigned long int inter;

int    gpib0,
        dev0,
        dev1,
        dev2,
        dev3;

struct data
 {
 unsigned long int number_point,
                                        numscan;
 float                  xincr,xmult,xzero,ymult,yzero;
 };

struct data info;

main()
 {
 introduction();
 init_parameter();
 init_device();
 init_files();
```

```
 measure();
 disable_device();
 }

void introduction()
 {
 _clearscreen(_GCLEARSCREEN);
 printf("\n\n\n\n ROWSCAN.C");
 printf("\n Collects RF data on a row.");
 printf("\n You can select the distance between two scanpoints (stepsize)");
 printf("\n and the total length of the row.\n");
 printf("\n Scaninformation will be stored in c:\\bti\\file_nam.dat");
 printf("\n Unscaled Values will be stored in c:\\bti\\file_nam.bin");
 }

void init_parameter()
 {
 static char fileout[5],
                        filenam[50]="c:\\bti\\",
                        intervall[3],
                        distance[20];

 unsigned long int dist;


 printf("\n Enter a 6 char output filename          : ");
 scanf("%s",fileout);
 strcat(filenam,fileout);
 strcpy(filebin,filenam);
 strcat(filebin,".bin");
 strcpy(filedat,filenam);
 strcat(filedat,".dat");
 printf(" Enter the scanaxis (1, 2 or 3)          : ");
 ax_number=getche();
 op=getche();
 printf("\n Enter the distance between collected waves: ");
 scanf("%s",intervall);
 printf(" Enter the length of the row in mm       : ");
 scanf("%s",distance);
 inter=atoi(intervall);
 dist=atoi(distance);
 info.numscan=(1000*dist/inter+1);
 printf("\n %u Scans of a row will be created.",info.numscan);
 switch(ax_number)
        {
```

```
        case'1':
                dev1=ibfind("axis1");
                strcpy(command, "MN A10 1V.01 D");
                strcat(command, intervall);
                strcat(command, " G ");
                strcpy(wait," 1R ");
                break;

        case'2':
                dev1=ibfind("axis2");
                strcpy(command, "MN A10 2V.01 D");
                strcat(command, intervall);
                strcat(command, " G ");
                strcpy(wait," 2R ");
                break;

        case '3':
                dev1=ibfind("axis3");
                strcpy(command, "MN A10 3V.01 D");
                strcat(command, intervall);
                strcat(command, " G ");
                strcpy(wait," 3R ");
                break;

        default:
                printf("\n unknown axis");
                op=getche();
                _clearscreen(_GCLEARSCREEN);
                exit(0);
        }
 }

void init_device(void)
 {
 static char trace[4],
                        output[12],
                        select[12];

 printf("\n\n Enter Trace (e.g. tra3)          : ");
 scanf("%s",trace);
 gpib0=ibfind("gpib0");
 dev0=ibfind("tekdev1");
 ibwrt(dev0,"DIG RUN ",8);
 strcpy(output,"OUTPUT ");
 strcpy(select,"SELECT ");
```

```
 strcat(output,trace);
 strcat(select,trace);
 printf("\n--%s--",output);
 printf("\n--%s--",select);

 ibwrt(dev0,output,strlen(output));

 ibwrt(dev0,select,strlen(select));
 ibwrt(dev0,"ENC WAV:bin ",12);
 ibwrt(dev0,"BYT LSB ",8);
 ibwrt(dev0,"ABB ON ",7);
 ibwrt(dev0,"WFM YMU:1 ",10);
 ibwrt(dev0,"WFM NR.pt:1024 ",14);
 ibwrt(dev0,"wfm?",4);
 ibrd(dev0,wfm,250);
 sscanf(wfm,"WFMPRE
ACSTATE:ENHANCED,NR.PT:%lu,PT.FMT:Y,XINCR:%g,XMULT:%g,XZERO:%g,
YMULT:%g,YZERO:%g",
 &info.number_point,&info.xincr,&info.xmult,&info.xzero,
 &info.ymult,&info.yzero);
 printf("\n\nPoints : %lu",info.number_point);
 printf("    Xincr : %g",info.xincr);
 printf("    Xmult : %g",info.xmult);
 printf("    Xzero : %g",info.xzero);
 printf("\nYmult  : %g",info.ymult);
 printf("    Yzero  : %g",info.yzero);
 printf("\n%s",wfm);
 ibwrt(dev1," F ",3);
 ibwrt(dev1," E ",3);
 }

void init_files()
 {

 if ((ptr_dat = fopen(filedat,"w")) == NULL)
        {
        printf(" error opening data file \n");
        exit(0);
        }

 if ((ptr_bin = fopen(filebin,"wb")) == NULL)
        {
        printf(" error opening binary file \n");
        exit(0);
        }
```

```
 fprintf(ptr_dat,"%g %g %g %lu %lu %g %g %lu",info.ymult,info.yzero,
 info.xincr,info.number_point,info.numscan,info.xmult,info.xzero,inter);
 fprintf(ptr_dat,"\nymult yzero xincr number_point numscan xmult xzero stepsize\n");
 fclose(ptr_bin);
 fclose(ptr_dat);
 }

void measure()
 {
 unsigned long int i,j,delay;
 static char curv[2060];

 if ((ptr_bin = fopen(filebin,"ab")) == NULL)
        {
        printf(" error appending to binary file \n");
        exit(0);
        }
 printf("\n\nPlease wait!!!  ");

 for(i=0;i<=(info.numscan-1);i++)
        {
        printf(".");
        ibwrt(dev0,"curve?",6);
  /*    for(delay=0;delay<=3500;delay++)
          {
          printf(".");
          }
        printf("/n->");  */
        ibrd(dev0,curv,2058);
        ibwrt(dev1, command, strlen(command));
        for (j=9;j<=2056;j++)
          {
          fputc(curv[j],ptr_bin);
          }
        while (asr[1] != 'R')
          {
          ibwrt(dev1,wait,strlen(wait));
          ibrd(dev1,asr,3);
          }
        asr[1] = 'B';

 }
 fclose(ptr_bin);
 }
```

```
void disable_device()
  {
  ibwrt(dev1, "F ",2);
  ibwrt(dev2, "F ",2);
  ibwrt(dev3, "F ",2);
  /* ibsic(gpib0);      */
  /* ibonl(gpib0,0); */
}
```

Program B.3. Rowscanb.bat
A batch file that takes the file, *rowscan.c* and outputs the following files, *rowscan.exe, rowscan.obj and rowscan.map*.

```
REM  rowscanb.bat 8/16/95
REM
cl /AL /c /O /Gs /Forowscan.obj rowscan.c
pause
link rowscan,rowscan,, c:\at-gpib\c\mcib+c:\qc2\lib\llibc7 /CO /STACK:16000 /SE:512
/MAP /NOE /NOD
pause
rowscan.exe
```

Program B.4. Corr.m

This *MatLab* file takes as input the two output files from *rowscan.exe*. The purpose of this program is to ascertain the speed of sound, c (whether longitudinal or shear) in a plate. Its outputs are two plots, one of the waveform and another, of the correlation coefficient, and the numerical values of the following parameters, the correlation coefficient *(Tx12)*, the sampling interval *(xincr)*, the time interval between echoes *(delta_t)* and the speed of sound *(c)*. This program, as presented below, assumes a 3/32 in. plate. If this is not true, the number, highlighted in bold in the program code below, will have to be changed to the correct plate thickness value. It also assumes that the data collected by *rowscan.exe* have the echo reflected off the near surface of the plate in the first 512 data point window, represented by T2, and the echo reflected off the far surface of the plate in the next 512 data point window, represented by T1.

```
% corr.m
% This function loads bin and dat file
% each A-Scanline is one column of matrix B

clear
n=input('Enter a filename : ','s');

bin=[n '.bin'];
dat=[n '.dat'];

fid=fopen(dat,'r');
A=fscanf(fid,'%f',[8,1]);
ymult=A(1,1);
yzero=A(2,1);
xincr=A(3,1);
number_point=A(4,1);
numscan=A(5,1);
xmult=A(6,1);
xzero=A(7,1);
stepsize=A(8,1);
status=fclose(fid);

fid=fopen(bin,'rb','g');
B=zeros(number_point,numscan);
B=fread(fid,[number_point,numscan],'short');
status=fclose(fid);

B=B';
B=B.*ymult;
B=B+yzero;

T1= B(1,:);
```

```
T2= B(1,:);

for i=512:1024
T1(i)=0;
end

for i=1:512
T2(i)=0;
end

Tx12= xcorr(T1,T2,'coeff');
[x,y] = max(Tx12)

figure
subplot(211)
plot(B(1,:));
subplot(212)
plot(Tx12);
ylabel('correlation coefficient')

xincr
delta_t=(y-number_point)*xincr
c= 2*3/32*2.54e-2/delta_t

clear n; clear bin; clear dat; clear fid; clear status; clear A;
```

Program B.5. b933.m

The purpose of this *Matlab* program is to calculate the spatial beat frequency of the Rayleigh surface wave on a plate, given the raw data supplied by the two output files from *rowscan.exe*. This file output two plots, one of the waveform and another, of the power spectrum of the waveform. The program code, as presented below, assumes a transmit frequency of 0.933 *MHz* and assumes the material is brass. If this is not so, the value of *px*, highlighted in bold, which is the theoretically predicted spatial beat frequency for brass at 0.933 *MHz*, will have to be altered. In this project, different material-transmit frequency case have their own individual version of this program, e.g., g700.m will mean a version of this program for glass-0.700 *MHz*.

```
% This function loads bin and dat file
% each A-Scanline is one column of matrix B

clear
n=input('Enter a filename : ','s');

bin=[n '.bin'];
dat=[n '.dat'];

fid=fopen(dat,'r');
A=fscanf(fid,'%f',[8,1]);
ymult=A(1,1);
yzero=A(2,1);
xincr=A(3,1);
number_point=A(4,1);
numscan=A(5,1);
xmult=A(6,1);
xzero=A(7,1);
stepsize=A(8,1);
status=fclose(fid);

fid=fopen(bin,'rb','g');
B=zeros(number_point,numscan);
B=fread(fid,[number_point,numscan],'short');
status=fclose(fid);

B=B';
B=B.*ymult;
B=B+yzero;

time = (xzero + xincr : xincr : xzero + number_point*xincr)*1e6;
distance = 1527*time*1e-6*100;

for tscan =1:numscan
```

```
rms(tscan) =0;
for counter = 1:number_point
int1(counter) = (real(B(tscan,counter)))^2;
end;
int2(tscan) = mean(int1);
rms(tscan) = (int2(tscan))^(1/2);
end;

ydistance = 0:stepsize/1000:stepsize/1000*(numscan-1);
figure;
subplot(211)
plot(ydistance,rms,'r');
ylabel('Amplitude(volts)');
xlabel('distance(mm)');

mrms = mean(rms);
nrms =  rms -mrms;
Y = fft(nrms,4096);
Pyy = Y .* conj(Y) / 4096;
f = (1/2e-4) * (0:2047) / 4096;
subplot(212)
plot(f,Pyy(1:2048),'r');
axis([0 100 0 1e-9])
py(1) = 0;
for i=1:1001
px(i)= 59.73;
py(i+1) = py(i)+ 1e-11;
end
hold
plot(px,py(1:1001),'y');
xlabel('frequency(Hz)');
ylabel('power spectrum');

%clear n;
clear bin;
clear dat;
clear fid;
clear status;
clear A;
```

APPENDIX C EXPERIMENTAL RESULTS

The following figures represent experimental results of measured beatlengths for five cases of aluminum, seven cases of brass and five cases of glass.

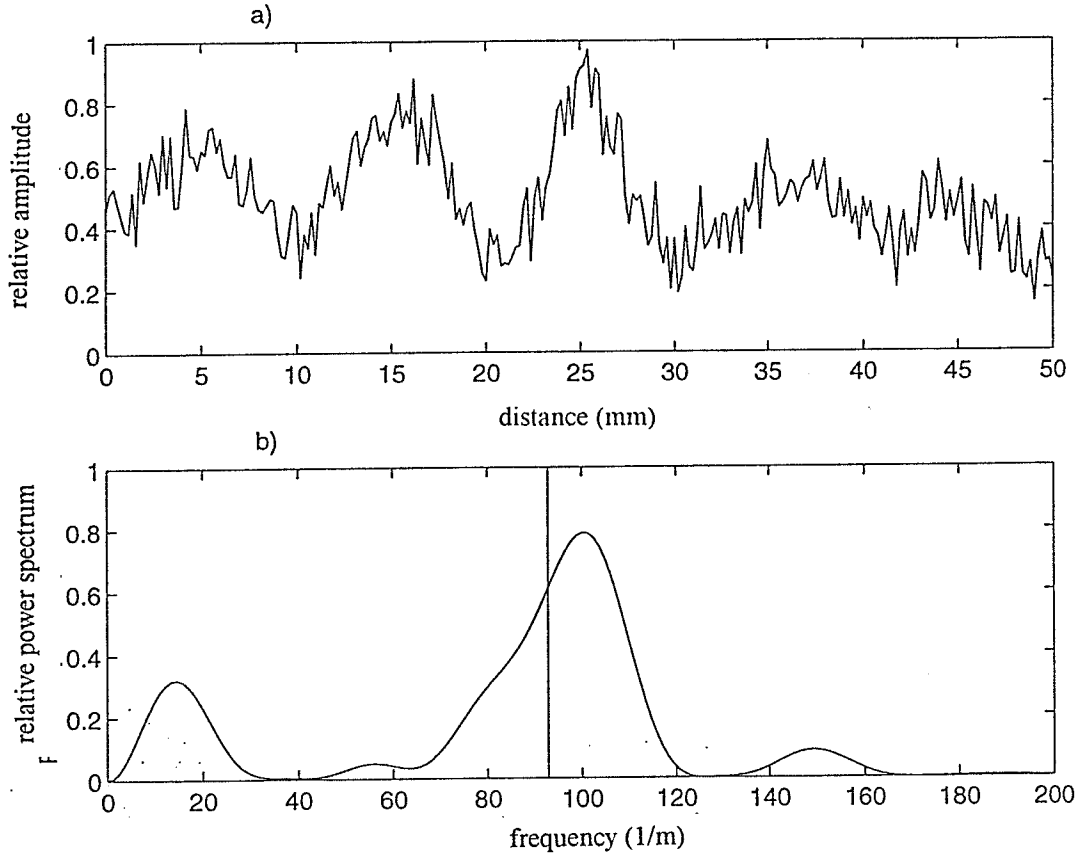

Figure C.1. (a) The spatially, amplitude modulated, received signal plotted against position along an aluminum plate's surface (250 RMS data points, 50 *mm* scan distance). (b) The power spectrum of the signal from (a) plotted against the spatial frequency (1/distance). The vertical line indicates the theoretically estimated spatial beat frequency, 92.9 m^{-1}. The frequency used was 1.2 *MHz*. The experimentally measured spatial beat frequency is 101.3 m^{-1}.

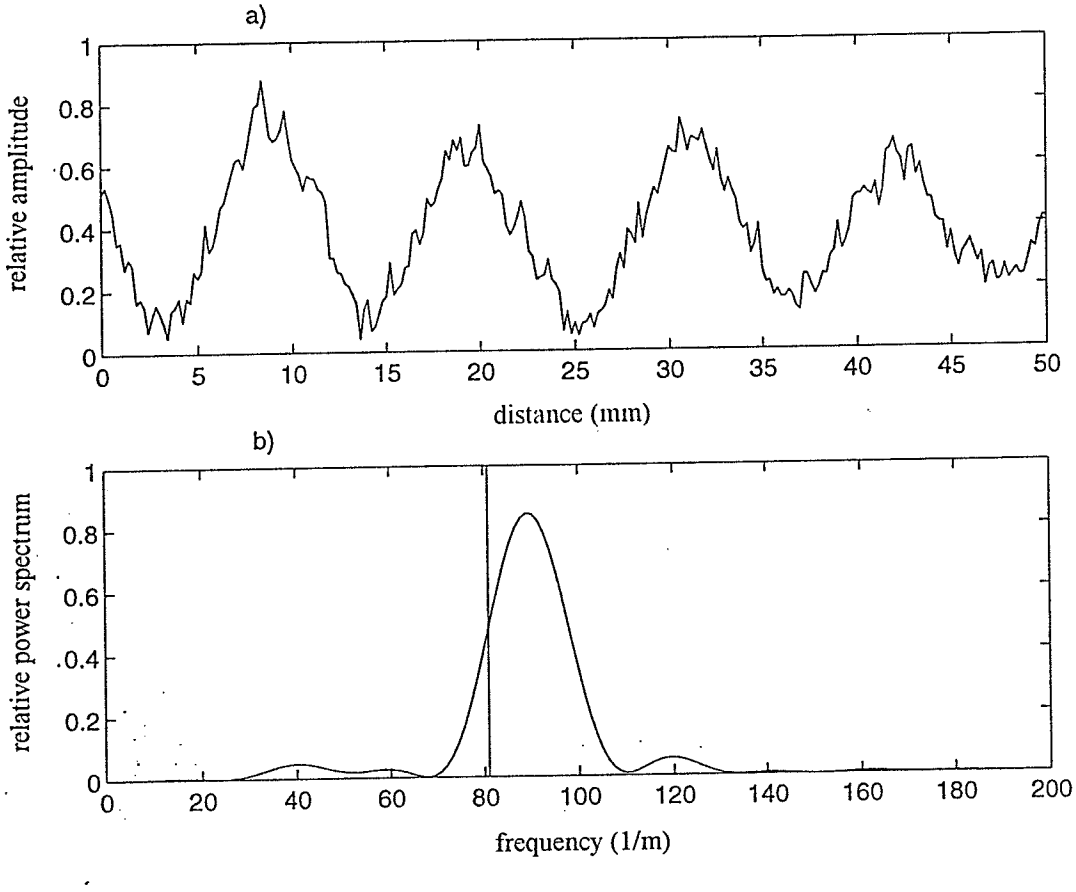

Figure C.2. (a) The spatially, amplitude modulated, received signal plotted against position along an aluminum plate's surface (250 RMS data points, 50 *mm* scan distance). (b) The power spectrum of the signal from (a) plotted against the spatial frequency (1/distance). The vertical line indicates the theoretically estimated spatial beat frequency, 80.9 m^{-1}. The frequency used was 1.26 *MHz*. The experimentally measured spatial beat frequency is 89.1 m^{-1}.

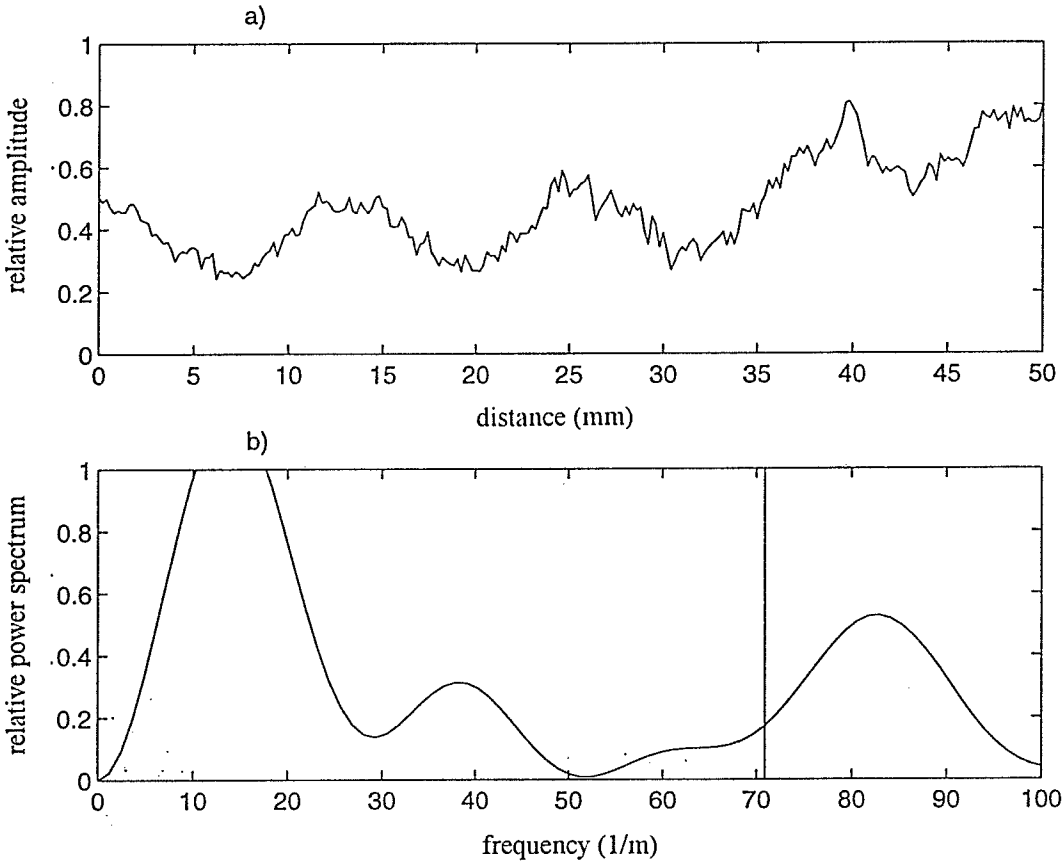

Figure C.3. (a) The spatially, amplitude modulated, received signal plotted against position along an aluminum plate's surface (250 RMS data points, 50 *mm* scan distance). (b) The power spectrum of the signal from (a) plotted against the spatial frequency (1/distance). The vertical line indicates the theoretically estimated spatial beat frequency, 70.9 m^{-1}. The frequency used was 1.33 *MHz*. The experimentally measured spatial beat frequency is 83.0 m^{-1}.

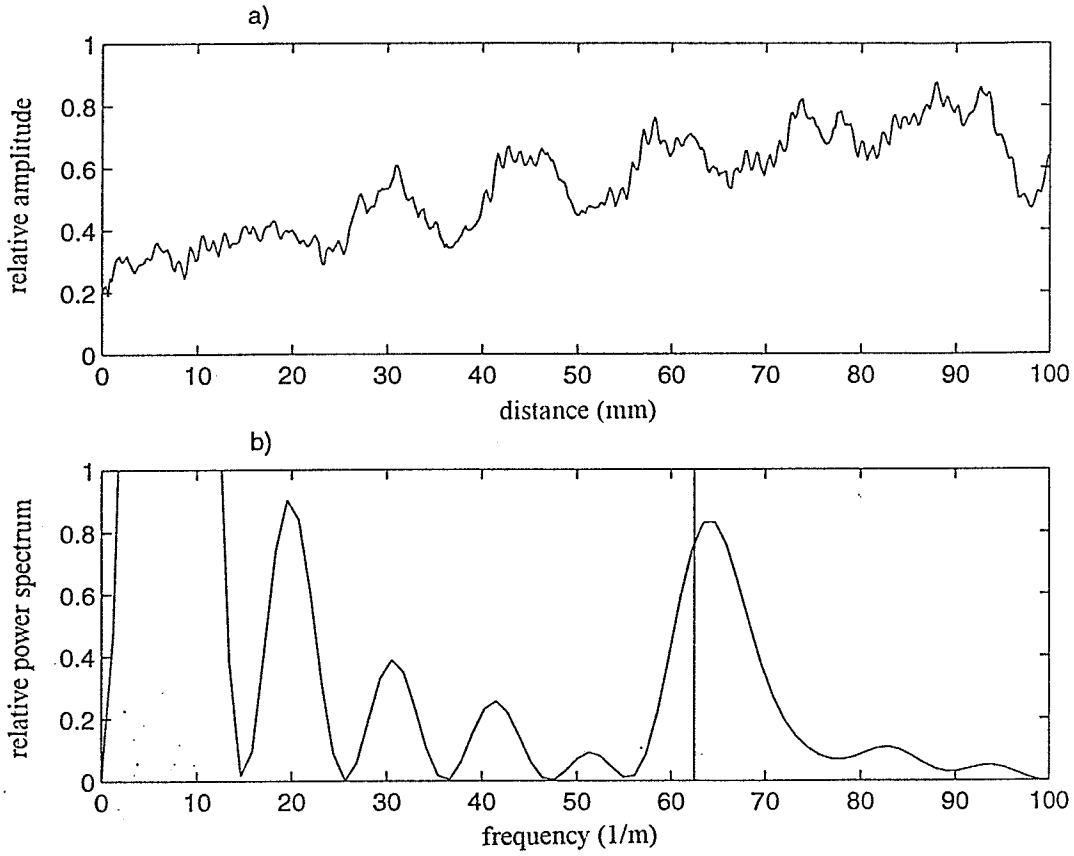

Figure C.4. (a) The spatially, amplitude modulated, received signal plotted against position along an aluminum plate's surface (500 RMS data points, 100 *mm* scan distance). (b) The power spectrum of the signal from (a) plotted against the spatial frequency (1/distance). The vertical line indicates the theoretically estimated spatial beat frequency, 62.5 m^{-1}. The frequency used was 1.4 *MHz*. The experimentally measured spatial beat frequency is 64.7 m^{-1}.

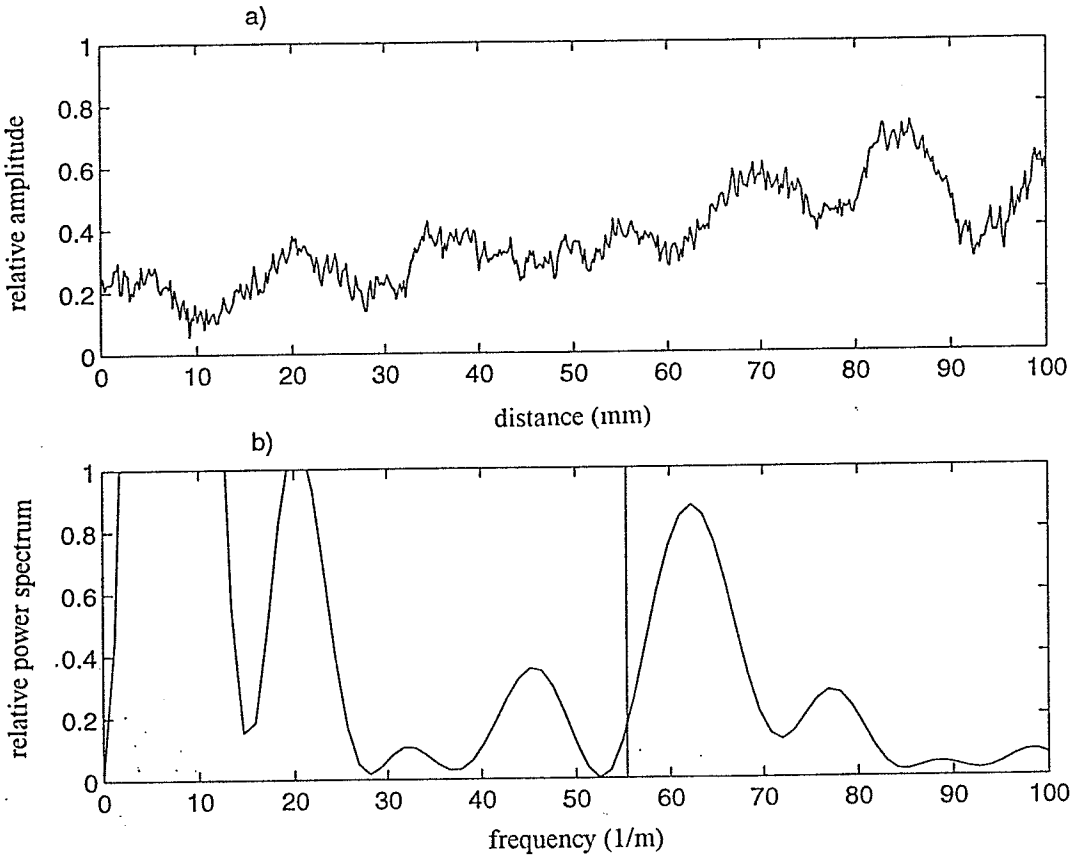

Figure C.5. (a) The spatially, amplitude modulated, received signal plotted against position along an aluminum plate's surface (500 RMS data points, 100 *mm* scan distance). (b) The power spectrum of the signal from (a) plotted against the spatial frequency (1/distance). The vertical line indicates the theoretically estimated spatial beat frequency, 55.4 m^{-1}. The frequency used was 1.46 *MHz*. The experimentally measured spatial beat frequency is 62.3 m^{-1}.

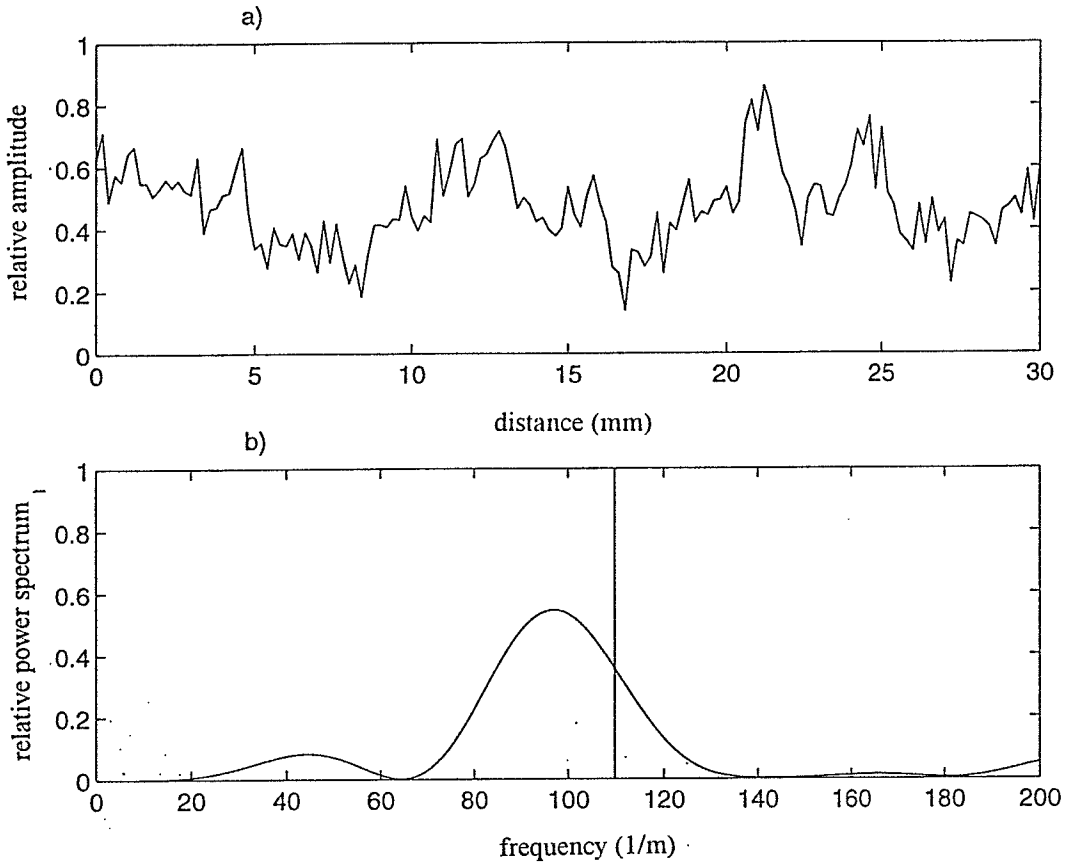

Figure C.6. (a) The spatially, amplitude modulated, received signal plotted against position along a brass plate's surface (150 RMS data points, 30 *mm* scan distance). (b) The power spectrum of the signal from (a) plotted against the spatial frequency (1/distance). The vertical line indicates the theoretically estimated spatial beat frequency, 109.8 m^{-1}. The frequency used was 0.73 *MHz*. The experimentally measured spatial beat frequency is 97.7 m^{-1}.

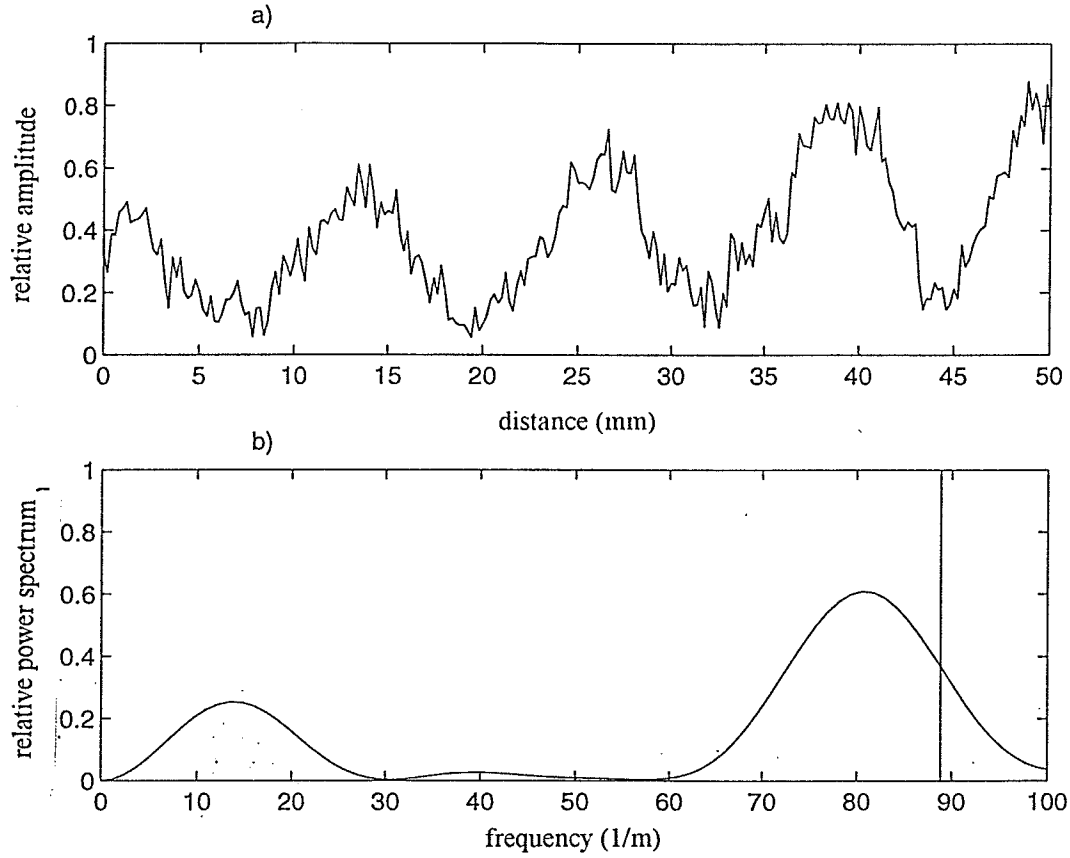

Figure C.7. (a) The spatially, amplitude modulated, received signal plotted against position along a brass plate's surface (250 RMS data points, 50 *mm* scan distance). (b) The power spectrum of the signal from (a) plotted against the spatial frequency (1/distance). The vertical line indicates the theoretically estimated spatial beat frequency, 88.9 m^{-1}. The frequency used was 0.80 *MHz*. The experimentally measured spatial beat frequency is 80.6 m^{-1}.

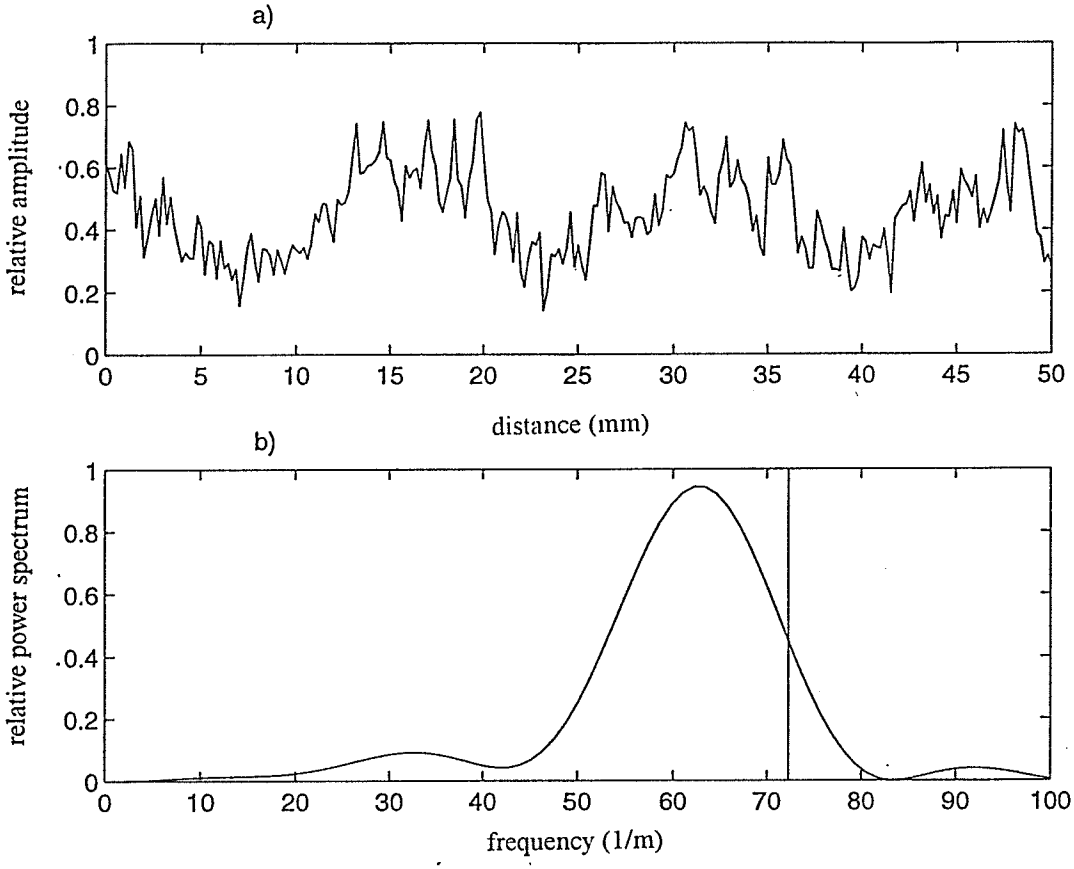

Figure C.8. (a) The spatially, amplitude modulated, received signal plotted against position along a brass plate's surface (250 RMS data points, 50 *mm* scan distance). (b) The power spectrum of the signal from (a) plotted against the spatial frequency (1/distance). The vertical line indicates the theoretically estimated spatial beat frequency, 72.3 m^{-1}. The frequency used was 0.86 *MHz*. The experimentally measured spatial beat frequency is 63.5 m^{-1}.

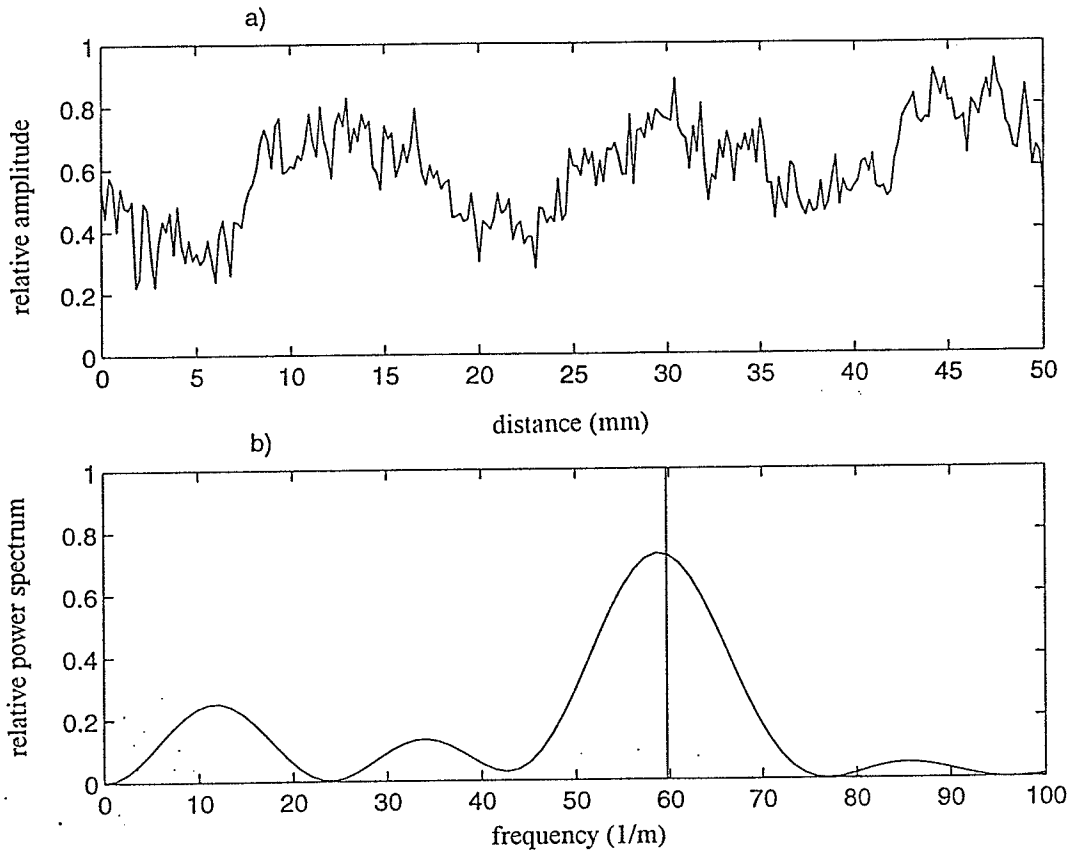

Figure C.9. (a) The spatially, amplitude modulated, received signal plotted against position along a brass plate's surface (250 RMS data points, 50 *mm* scan distance). (b) The power spectrum of the signal from (a) plotted against the spatial frequency (1/distance). The vertical line indicates the theoretically estimated spatial beat frequency, 59.7 m^{-1}. The frequency used was 0.93 *MHz*. The experimentally measured spatial beat frequency is 58.6 m^{-1}.

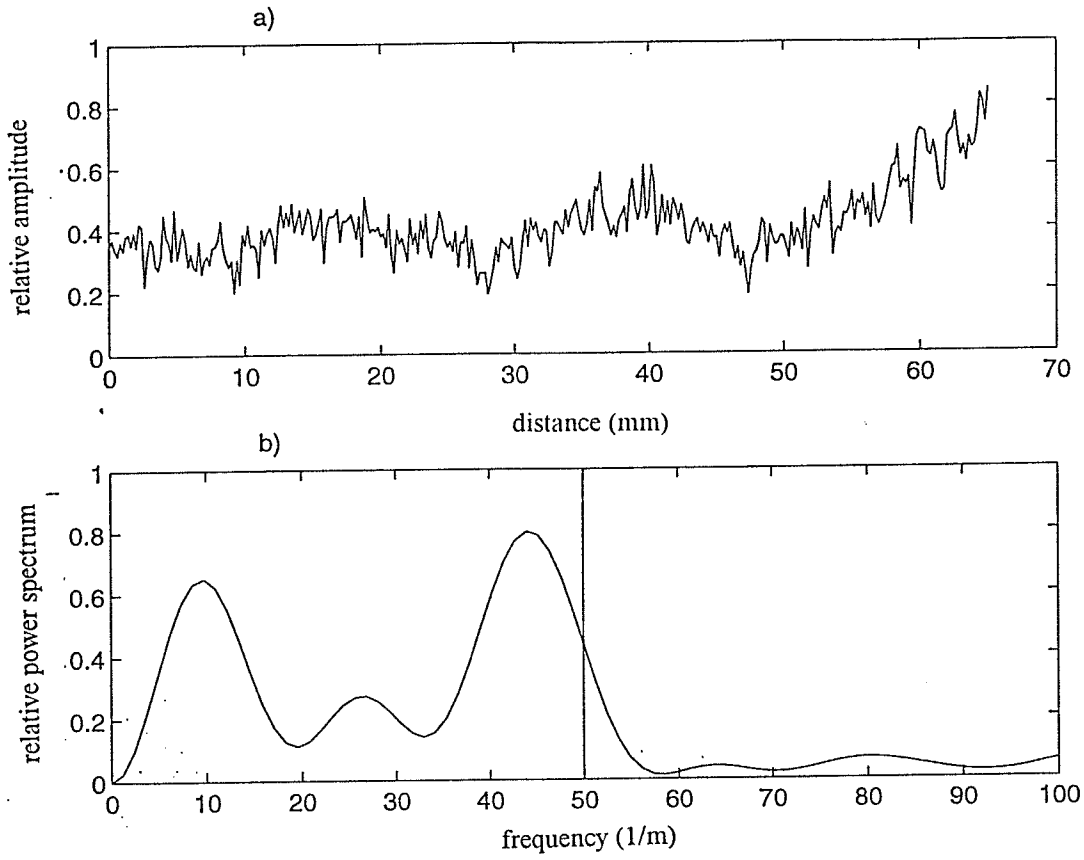

Figure C.10. (a) The spatially, amplitude modulated, received signal plotted against position along a brass plate's surface (350 RMS data points, 70 *mm* scan distance). (b) The power spectrum of the signal from (a) plotted against the spatial frequency (1/distance). The vertical line indicates the theoretically estimated spatial beat frequency, 50.0 m^{-1}. The frequency used was 1.00 *MHz*. The experimentally measured spatial beat frequency is 45.2 m^{-1}.

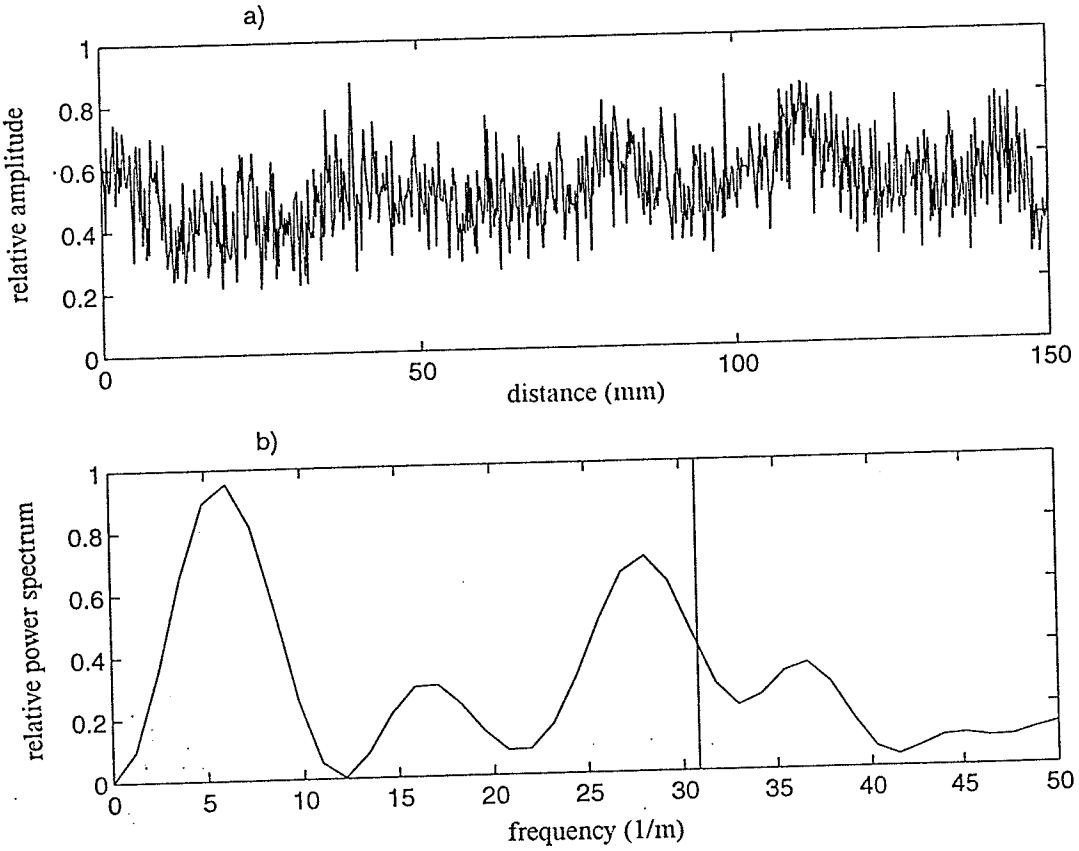

Figure C.11. (a) The spatially, amplitude modulated, received signal plotted against position along a brass plate's surface (750 RMS data points, 150 *mm* scan distance). (b) The power spectrum of the signal from (a) plotted against the spatial frequency (1/distance). The vertical line indicates the theoretically estimated spatial beat frequency, 30.8 m^{-1}. The frequency used was 1.20 *MHz*. The experimentally measured spatial beat frequency is 28.1 m^{-1}.

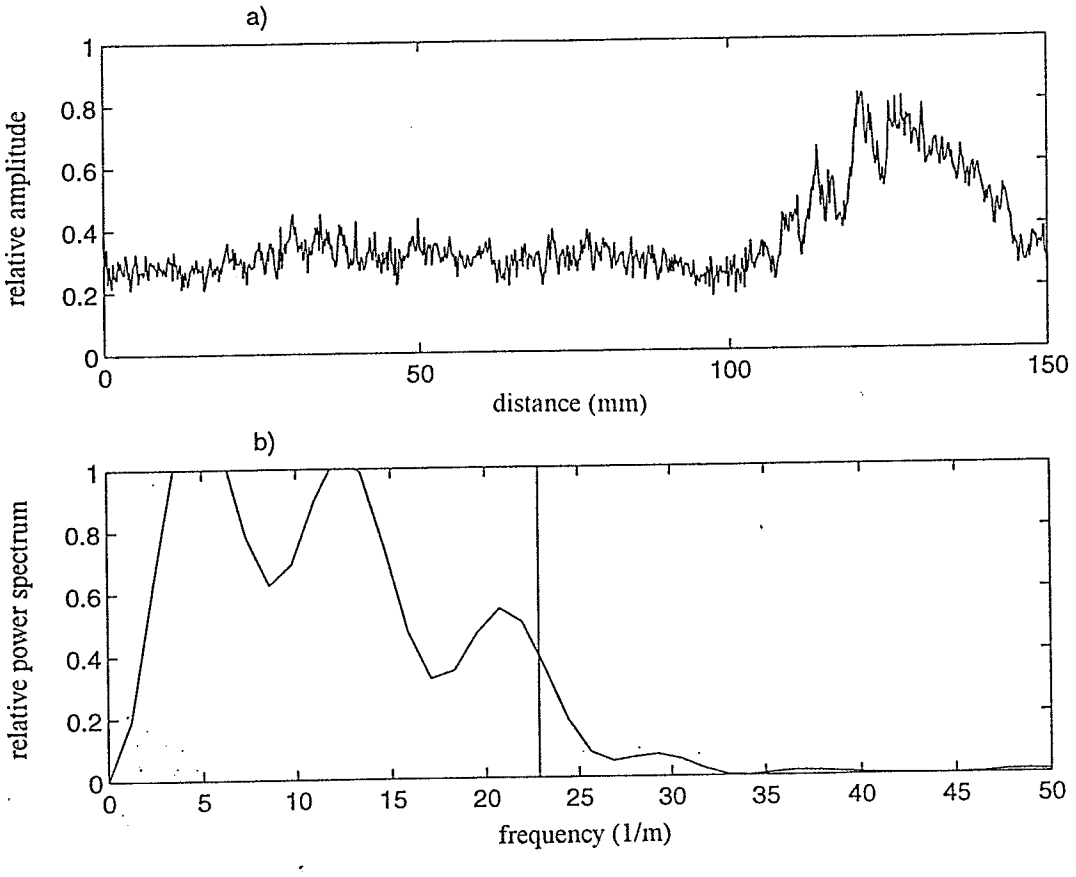

Figure C.12. (a) The spatially, amplitude modulated, received signal plotted against position along a brass plate's surface (750 RMS data points, 150 *mm* scan distance). (b) The power spectrum of the signal from (a) plotted against the spatial frequency (1/distance). The vertical line indicates the theoretically estimated spatial beat frequency, 22.9 m^{-1}. The frequency used was 1.33 *MHz*. The experimentally measured spatial beat frequency is 22 m^{-1}.

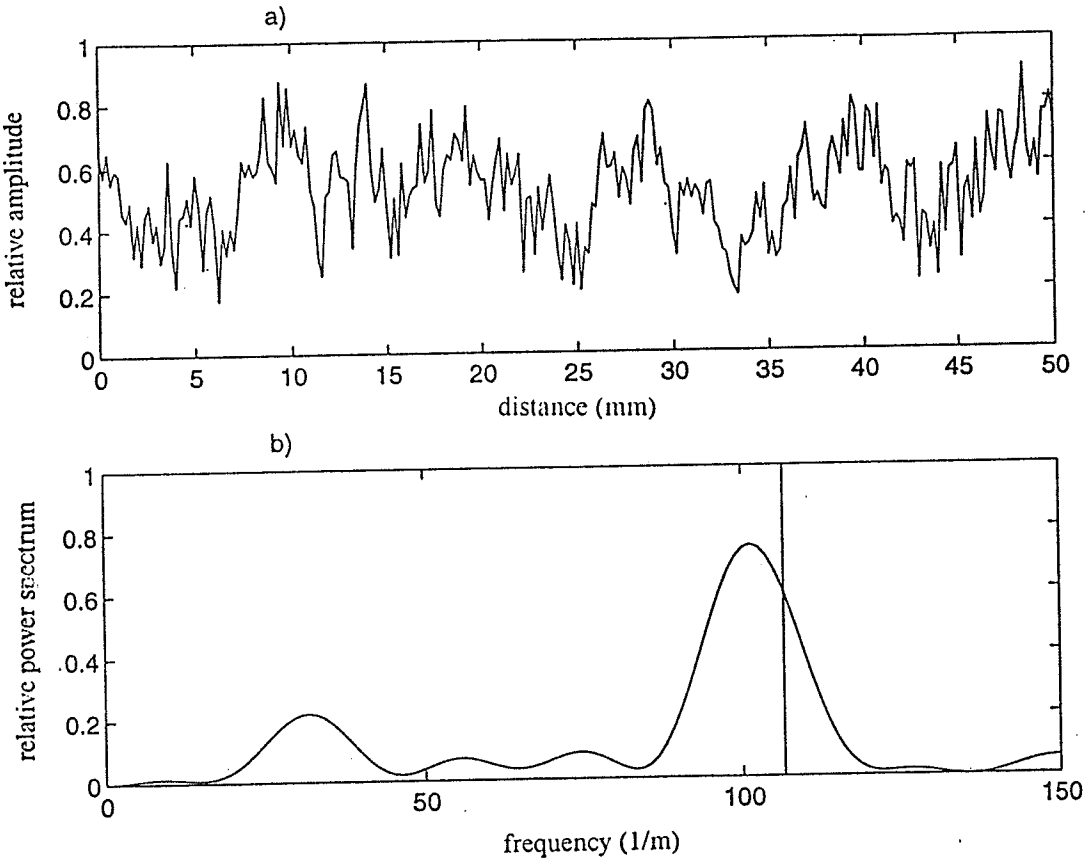

Figure C.13. (a) The spatially, amplitude modulated, received signal plotted against position along a glass plate's surface (250 RMS data points, 50 *mm* scan distance). (b) The power spectrum of the signal from (a) plotted against the spatial frequency (1/distance). The vertical line indicates the theoretically estimated spatial beat frequency, 106.5 m^{-1}. The frequency used was 0.70 *MHz*. The experimentally measured spatial beat frequency is 101.3 m^{-1}.

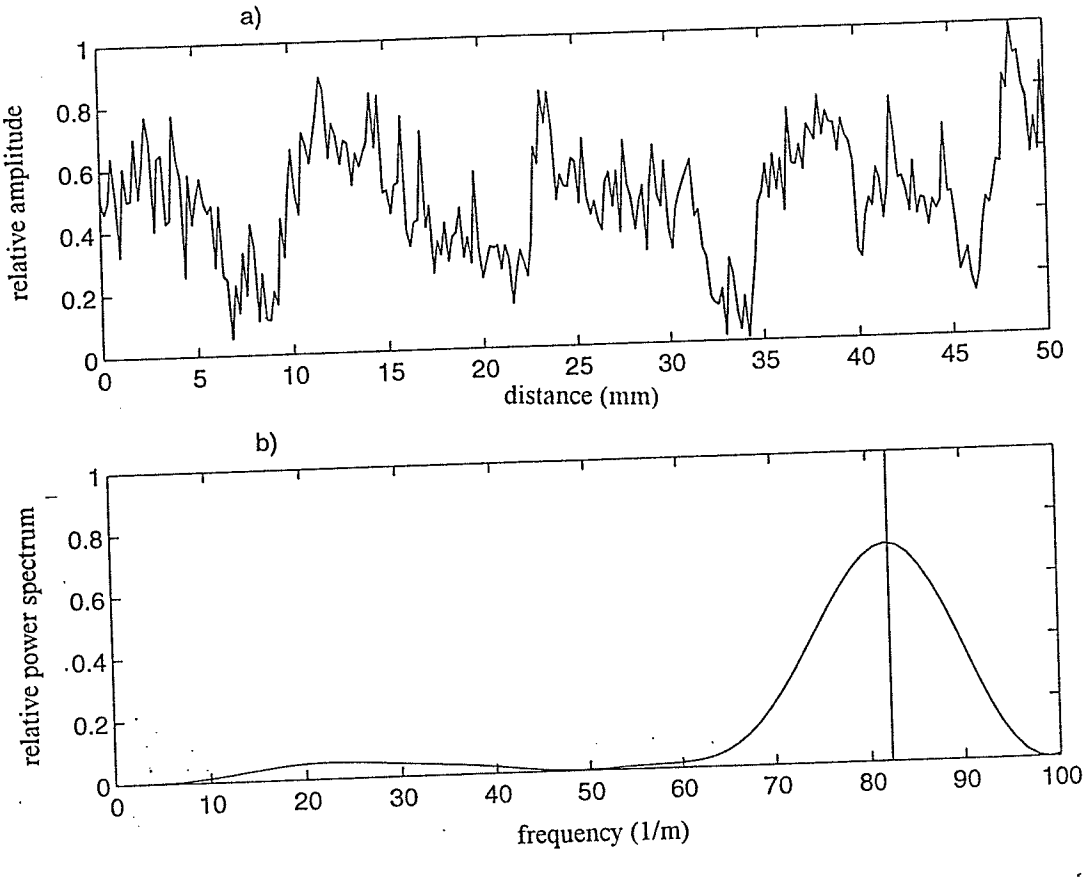

Figure C.14. (a) The spatially, amplitude modulated, received signal plotted against position along a glass plate's surface (250 RMS data points, 50 *mm* scan distance). (b) The power spectrum of the signal from (a) plotted against the spatial frequency (1/distance). The vertical line indicates the theoretically estimated spatial beat frequency, 82.2 m^{-1}. The frequency used was 0.80 *MHz*. The experimentally measured spatial beat frequency is 81.8 m^{-1}.

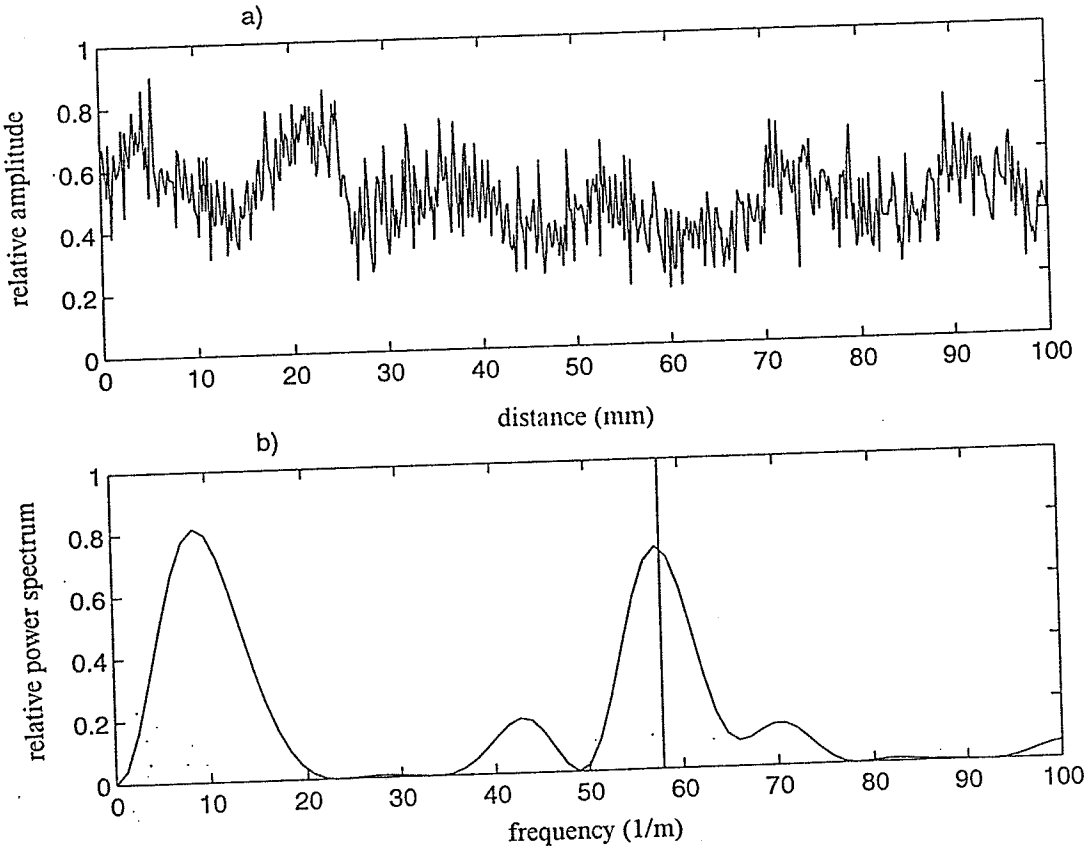

Figure C.15. (a) The spatially, amplitude modulated, received signal plotted against position along a glass plate's surface (500 RMS data points, 100 *mm* scan distance). (b) The power spectrum of the signal from (a) plotted against the spatial frequency (1/distance). The vertical line indicates the theoretically estimated spatial beat frequency, 57.9 m^{-1}. The frequency used was 0.90 *MHz*. The experimentally measured spatial beat frequency is 57.4 m^{-1}.

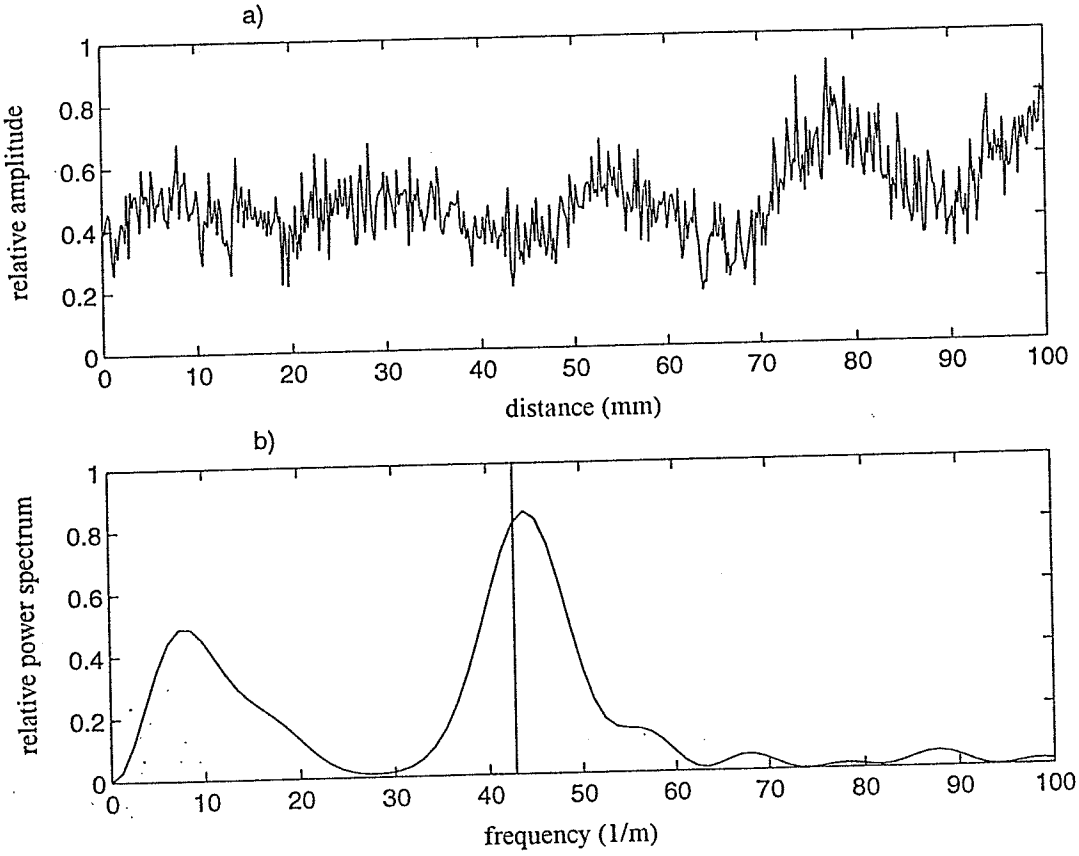

Figure C.16. (a) The spatially, amplitude modulated, received signal plotted against position along a glass plate's surface (500 RMS data points, 100 *mm* scan distance). (b) The power spectrum of the signal from (a) plotted against the spatial frequency (1/distance). The vertical line indicates the theoretically estimated spatial beat frequency, 42.9 m^{-1}. The frequency used was 1.00 *MHz*. The experimentally measured spatial beat frequency is 44.0 m^{-1}.

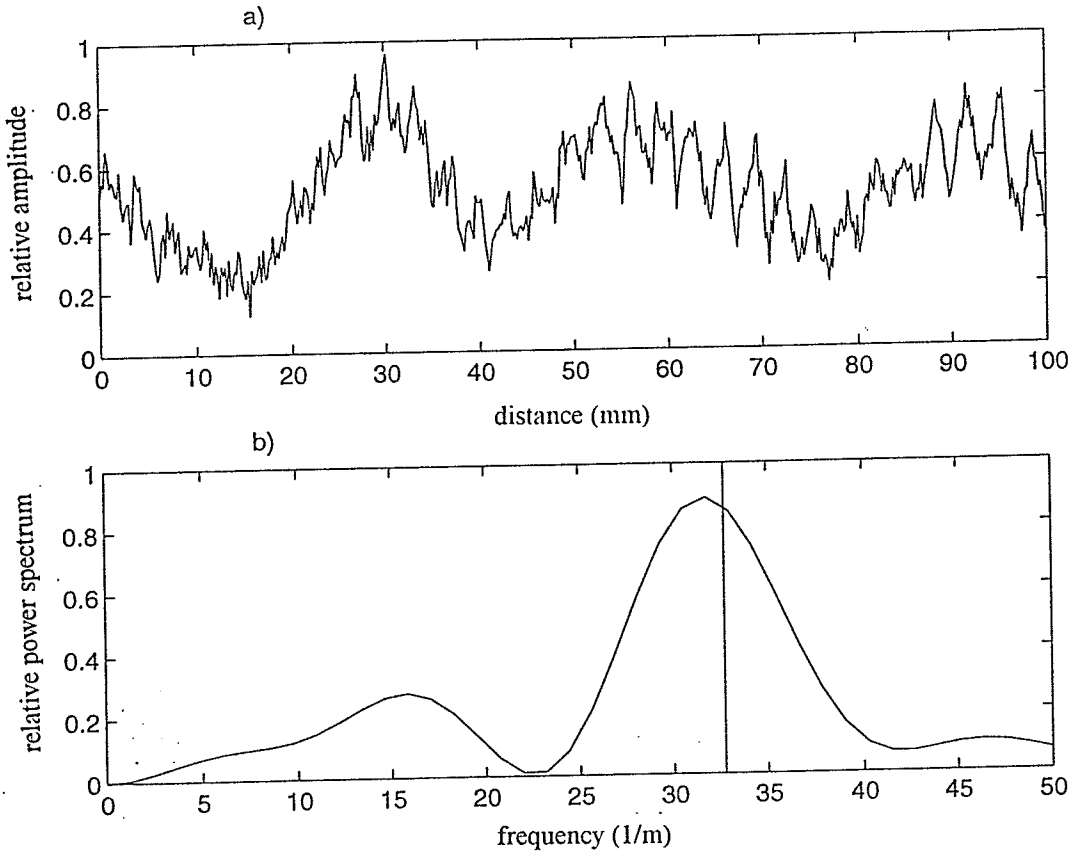

Figure C.17. (a) The spatially, amplitude modulated, received signal plotted against position along a glass plate's surface (500 RMS data points, 100 *mm* scan distance). (b) The power spectrum of the signal from (a) plotted against the spatial frequency (1/distance). The vertical line indicates the theoretically estimated spatial beat frequency, 32.7 m^{-1}. The frequency used was 1.10 *MHz*. The experimentally measured spatial beat frequency is 31.7 m^{-1}.

LIST OF REFERENCES

[1] B.A. Auld, *Acoustic Fields and Waves in Solids*, vol. 2. Malabar, FL: Krieger, 1990.

[2] I.A. Viktorov, *Rayleigh and Lamb Waves*. NY: Plenum Press, 1967.

[3] L. Brekhovskikh and V. Goncharov, *Mechanics of Continua and Wave Dynamics*. NY: Springer, 1985. Note that the first of Eqs. (5.16) has a sign error. The plus sign between the two terms should be replaced by a minus sign.